

Lanthanoid complexes of cyclopentadienyl ligands

Master's thesis

University of Jyväskylä

Department of Chemistry

Inorganic chemistry department

09.05.2019

Teemu Mäkelä

Abstract

Lanthanoid (Ln) complexes are usually studied, because of four main reasons: fundamental interest on lanthanoid chemistry, luminescent properties, catalytic capabilities and magnetic properties. Research on magnetic properties of lanthanoid complexes has led to group of complexes that show slow relaxation of magnetization of purely molecular origin in low temperatures. Such complexes are called lanthanoid single molecular magnets (Ln-SMM). Recently, lanthanoids have dominated the development of new SMMs over the transition metals. Anisotropy of lanthanoid ion and the ligand field geometry around the ion are the main things affecting on the magnetic properties of the complex. Most successful metal-ligand combination in the field of Ln-SMMs has been dysprosium metallocenium unit $[(C_5R_5)_2Dy]^{n+}$. This thesis gives a short introduction to the magnetic capabilities and synthetic matters of lanthanoid complexes based on cyclopentadienyl ligands.

This thesis consists of the literature part and experimental part. First in the literature part basic concepts and theory about lanthanoids, cyclopentadienyls and single molecular magnetism are presented shortly. Then mononuclear complexes will be discussed starting from the development and potential of divalent lanthanoid ions (M^{2+}) in the complexes of cyclopentadienyl ligands. Trivalent lanthanoid ions (M^{3+}) in the mononuclear cyclopentadienyl complexes are also dealt with before discussing the polynuclear complexes, which are divided in two groups. The first group includes complexes with bridging ligands that have heteroatoms as donor atoms, whereas the second group focuses the hydride bridged complexes. The main emphasis is on the latest achievements in each field, but development of the complexes is also discussed.

In the experimental part, the syntheses and reductions of dinuclear rare-earth metal complexes with the redox active bridging ligand are discussed. Due to the results of experimental part will be published in the peer-reviewed scientific journal, they will be published in *JYX* after they are accepted for the publication because of prior publication policies of scientific journals.

Tiivistelmä

Lantanoidikomplekseja on tutkittu pääasiassa neljästä syystä, joita ovat fundamentaalinen kiinnostus lantanoidikemiaan, lantanoidien luminesenssi, niiden katalyyttinen kyvykyys ja magneettiset ominaisuudet. Lantanoidien magneettisten ominaisuuksien tutkimus on johtanut joukkoon komplekseja, joissa on havaittavissa molekyylistä itsestään johtuvaa magnetisaation hidasta relaksoitumista alhaisissa lämpötiloissa. Tällaisia komplekseja kutsutaan lantanoidi-yksittäismolekyylimagneeteiksi (Ln-SMM). Viime aikoina lantanoidit ovat hallinneet uusien yksittäismolekyylimagneettien kehitystä transitionmetallien sijaan. Lantanoidi-ionin anisotropia ja ionia ympäröivän ligandikentän geometria ovat pääasialliset lantanoidikompleksien magneettisiin ominaisuuksiin vaikuttavat tekijät. Kaikkein onnistuneimmat metalli-ligandi yhdistelmät Ln-SMM:ien alalla ovat olleet dysprosiumin metallooseeni yksiköt $[(C_5R_5)_2Dy]^{n+}$. Tämä tutkielma antaa lyhyen esittelyn lantanoidikompleksien magneettisiin ominaisuuksiin ja synteettisiin seikkoihin.

Tämä tutkielma koostuu kirjallisuusosasta ja kokeellisesta osasta. Kirjallisuusosassa käydään ensin lyhyesti läpi perusasioita ja teoriaa lantanoideista, syklopentadieeneistä ja yksittäismolekyylimagnetismista. Seuraavaksi käsitellään yksiytimisiä komplekseja alkaen divalenttien lantanoidikompleksien (M^{2+}) kehityksestä ja niiden kemiallisista ja magneettisista mahdollisuuksista. Trivalenttien lantanoidien (M^{3+}) yksiytimisiä komplekseja käydään myös läpi ennen siirtymistä moniytimisiin lantanoidikomplekseihin, jotka on jaettu kahteen ryhmään. Ensimmäiseen ryhmään kuuluvat kompleksit, joiden siltaavat ligandit sisältävät heteroatomeja, kun taas toinen sisältää komplekseja siltaavilla hydridiligandeilla. Pääpaino on kunkin alan uusimmissa saavutuksissa, mutta myös kompleksien kehitystä käydään läpi.

Kokeellisessa osiossa käydään läpi kaksiytimisten redox-aktiivisella ligandilla sillattujen harvinaisten maametallien kompleksien synteesejä ja pelkistysreaktioita. Kokeellisen osion tulokset on tarkoitus julkaista vertaisarvioidussa tieteellisessä lehdessä, jonka takia ne toimitetaan *JYX*:iin vasta julkaisuprosessin jälkeen julkaisutalojen julkaisukäytännöistä johtuen.

Preface

This Master's thesis was written between March of 2018 and April of 2019. The experimental work was performed between October of 2017 and March of 2018 in University of Jyväskylä in the Main Group Chemistry research group. In information retrieval the articles were sought mainly by using SciFinder, Reaxys, Google Scholar and material retrieval system of Jyväskylä University's library (JYKDOK).

First, I want to thank my supervisor and mentor Jani Moilanen, who has supported me through the whole process from experimental work to finishing the whole thesis. He offered me an opportunity to perform the experimental work about dinuclear lanthanoid complexes as his assistant and working with him has been inspiring. I thank him also for being my instructor during the experimental work and for measuring and solving all of the crystal structures in the experimental part of the thesis. I also wish to thank Jari Konu for being the other reviewer of this thesis. I want to express my gratitude to professor Heikki Tuononen for letting me to do the thesis in his research group and great thanks to all members of the Main Group Chemistry research group, who have helped and advised me during the experimental work. I thank Academy of Finland for the financial support on the experimental research.

Lahti, 29.04.2019

Teemu Mäkelä

Table of Contents

ABSTRACT	II
TIIVISTELMÄ.....	III
PREFACE.....	IV
ABBREVIATIONS	VI
1. INTRODUCTION.....	1
2. THEORETICAL BACKGROUND.....	2
2.1. BASICS ABOUT LANTHANOIDS AND THEIR COMPLEXES	2
2.2. CYCLOPENTADIENYLS AS LIGANDS	4
2.3. BASICS OF LANTHANOID SINGLE MOLECULAR MAGNETS.....	5
3. LANTHANOID COMPLEXES WITH CYCLOPENTADIENYL LIGANDS.....	8
3.1. DIVALENT MONONUCLEAR COMPLEXES.....	8
3.1.1. Synthesis of the whole series	8
3.1.2. Determination of electronic configurations	10
3.1.3 Other complexes of divalent lanthanoids.....	12
3.2. TRIVALENT MONONUCLEAR COMPLEXES	13
3.2.1. Synthetic capabilities of [Cp* ₂ M][BPh ₄].....	14
3.2.2. Low coordinated complexes	16
3.3. POLYNUCLEAR HETEROATOM BRIDGED COMPLEXES.....	18
3.3.1. N-bridged complexes	18
3.3.2. Dinuclear complexes with various bridging ligands.....	25
3.3.3. Trinuclear Ln-SMM s with pnictogen donor ligands	29
3.4. POLYNUCLEAR HYDRIDE BRIDGED COMPLEXES	32
4. CONCLUSIONS.....	38
LIST OF REFERENCES	40

Abbreviations

BPh₄ = tetraphenylborate, B(C₆H₆)₄

bpym = 2,2'-bipyrimidine, C₈H₆N₄

btaH = 1H-1,2,3-benzotriazole

Cp = Cyclopentadienyl, [C₅H₅]⁻

Cp^{iPr5} = Penta-isopropylcyclopentadienyl, [C₅(CH(CH₃)₂)₅]⁻

Cp^{Me} = Methylcyclopentadienyl, [C₅H₄(CH₃)]⁻

Cp^{Me4} = Tetramethylcyclopentadienyl, C₅H(CH₃)₄

Cp^{SiMe3} = Trimethylsilylcyclopentadienyl, [C₅H₄(Si(CH₃)₃)]⁻

Cp^{(SiMe3)2} = di(trimethylsilyl)cyclopentadienyl, [C₅H₃(Si(CH₃)₃)_{2-1,3}]⁻

Cp^{ttt} = Tri-*tert*-butylcyclopentadienyl, [C₅H₂(C(CH₃)₃)_{3-1,2,4}]⁻

Cp* = Pentamethylcyclopentadienyl, [C₅(CH₃)₅]⁻

EPR = Electron spin resonance

J = Exchange coupling constant

Ln = Lanthanoids

Ln-Cp complexes = Lanthanoid complexes of cyclopentadienyl ligands

Ln-SMM = Lanthanoid-based single molecular magnet

M = La, Ce, Pr, Nd, Pm, Sm, Eu, Gd, Tb, Dy, Ho, Er, Tm, Yb, Lu or Y

M-Cnt distance = distance between the metal ion and centroid of the cyclopentadienyl ring

NMR = Nuclear magnetic resonance

n-BuLi = Lithium-1-butanide (CH₃(CH₂)₃Li)

SCXRD = Single Crystal X-Ray Diffractometry

SQUID = Superconducting quantum interference device

T_b = Magnetic blocking temperature

tppz = 2,3,5,6-tetra(2-pyridyl)pyrazine, C₂₄H₁₆N₆

τ = Time of magnetic relaxation

U_{eff} = Magnetic anisotropy barrier / spin relaxation barrier

[2.2.2]Cryptand, crypt-222 = 4,7,13,16,21,24-Hexaoxa-1,10-diazabicyclo[8.8.8]hexacosane

18-crown-6 = 1,4,7,10,13,16-Hexaoxacyclooctadecane

1. Introduction

Lanthanoid complexes of cyclopentadienyl (Cp) ligands have been known for over 60 years.¹ During the time, Cp- ligands have proved their versatility in lanthanoid complexes again and again. Cp- ligands offer synthetic versatility in lanthanoid complexes, because they can be easily substituted with other coordinating ligands. Cp- ligands can also be modified with various functional groups. This makes possibilities of Cp- ligands almost limitless. However, group of Cp- ligands usually used in lanthanoid complexes is constricted to some extent, because of the complex nature of lanthanoids.

Today majority of lanthanoid research is focused on magnetic properties of lanthanoid complexes and on single molecular magnetism. SMMs are molecular species that show the slow relaxation of magnetization in low temperatures. Lanthanoid complexes have shown their capability in single molecular magnetism and so far, the best SMMs created are dysprosium metallocenium complexes.²⁻⁴ Especially for multinuclear lanthanoid SMMs (Ln-SMM) with coupling interactions between magnetic cores, theory tends to lag experimental results. Therefore, magnetic properties of multinuclear complexes are difficult to predict beforehand. Also, dynamic magnetic properties of Ln-SMMs cannot be explained with current theoretical knowledge. The best results have been accomplished with right kind of ligand field geometry that boosts the strong single ion anisotropy of Ln ion. For example, the strong axial and weak equatorial ligand field for Dy³⁺- ion.⁵

Basic theoretical aspects of Lanthanoids, Cp- ligands and Ln-SMMs are briefly presented in next chapter and after that different types of lanthanoid-Cp complexes are reviewed, and their synthetic and magnetic aspects are discussed. The literature part ends with conclusions, where main points of all categories are concluded.

2. Theoretical background

For clarification, in this thesis the term “lanthanoid” refers to elements La - Lu, even though lanthanum is a d-block metal and not an f-block metal like elements Ce - Lu. La can be considered as one of the lanthanoids, because of its similarity in chemical properties with f-block lanthanoids. La has electronic configuration of $[\text{Xe}]6s^25d^1$, which resembles electronic configurations of f-block lanthanoids, and it prefers oxidation state of +3 like f-block lanthanoids do. Only difference between La and f-block lanthanoids is that La has an empty 4f- orbital.⁶

2.1. Basics about lanthanoids and their complexes

The chemistry of lanthanoid complexes is strongly related to 4f- electron shell. Characteristic phenomenon for f-block lanthanoids and lanthanum is called lanthanoid contraction. The simple explanation for lanthanoid contraction is steady decrease in radii of lanthanoid atoms and ions from La to Lu across the whole series. The phenomenon is particularly clear with M^{3+} - ions of lanthanoids, because M^{3+} ions do not have any 6s or 5d electrons. The same contraction is also observed with elements Hf - Hg on third row of d- block elements in the periodic table of elements. The lanthanoid contraction is caused by imperfect shielding of 4f- electrons. The shielding of increasing number of electrons is less prominent than the increasing positive charge of the nucleus. The result is increase in the effective nuclear charge from La to Lu causing 4f- electrons to lie closer to the nucleus in heavier lanthanoids. For comparison, in d-block metals electrons on d- orbitals shield each other more efficiently from the charge of the nucleus. Being contracted species that contain a lot of electrons also means that lanthanoid ions have a lot of electron density on themselves. Therefore, coordination bonds between lanthanoid ions and ligands are usually ionic. Ionic nature of lanthanoid complexes is usually emphasized by marking lanthanoid complexes as ionic species like $[\text{M}][\text{L}]$, where L = ligand.⁶

The most typical oxidation state for lanthanoids is +3. +4 oxidation states are rare for lanthanoids, because of contracted nature of 4f- orbitals. The exception to this is cerium that has tendency to form Ce^{4+} - ions with empty 4f- shell. +2 oxidation states are available for all lanthanoids in specific coordination environments, as discussed later in this thesis.⁷ Limited number of possible oxidation states makes it easier to for example reduce specific ligands in lanthanoid complexes to stable radicals without affecting the oxidation state of Ln ions. Lanthanoid complexes have wide range of possible coordination numbers. Lanthanoid ions

have large ionic radii, which is why the high coordination numbers are typical. Low coordination numbers require use of carefully selected bulky ligands.⁶

Lanthanoids are notoriously oxophilic elements, which means that oxygen coordinates strongly to lanthanoid ions. Oxophilicity makes most of the lanthanoid complexes air- and moisture sensitive. Because of their sensitivity, lanthanoid complexes are usually synthesized and examined under an inert atmosphere using specific techniques like Schlenk line and an inert atmosphere glove box. Water is a coordinating solvent, but oxophilicity makes lanthanoid complexes vulnerable also to other coordinating solvents containing oxygen atoms like tetrahydrofuran (THF). THF is not only difficult to remove from lanthanoid complexes, which makes THF a tricky solvent, but THF has also its benefits in lanthanoid chemistry, because sometimes THF helps in crystallization of lanthanoid complexes. Good crystals of lanthanoid complexes are essential in determining their crystal structures with single crystal X-ray diffraction (SCXRD), which is important technique in characterization of paramagnetic lanthanoid complexes.⁶

Yttrium is not a lanthanoid, but it is often used concurrently with lanthanoids in series of complexes. Scandium, yttrium and lanthanoids together are called rare-earth metals. Y is used with lanthanoids, because its chemical properties are very similar to the chemical properties of lanthanoids. Y is also oxophilic like lanthanoids. Ionic radii 1.019 Å of eight coordinate Y^{3+} - ion is close to radii 1.015 Å of eight coordinate Ho^{3+} - ion.⁸ In complexes Y is usually on oxidation state of +3, but in specific coordination environments oxidation state of +2 is also available.⁹ Complexes synthesized with Y can usually be synthesized also with lanthanoids that have radius close to radius of Y. One benefit of using Y^{3+} in complexes in place of Ln is that Y^{3+} is a diamagnetic ion contrast to paramagnetic +3 lanthanoids ions (Ce^{3+} , Nd^{3+} , Sm^{3+} , Gd^{3+} , Dy^{3+} , Er^{3+} , Yb^{3+}). Unlike paramagnetic complexes, diamagnetic complexes can be characterized by nuclear magnetic resonance (NMR) spectroscopy unambiguously. Diamagnetic nature of Y complexes is also beneficial in electron spin resonance (EPR) spectroscopy, when complexes with radical ligands are synthesized. Diamagnetic starting material does not show signal in EPR measurement, but radical product does. Y^{3+} is also used in multinuclear Ln-SMMs as magnetically dilute complexes, where all but one Ln^{3+} are replaced with Y^{3+} , are synthesized.¹⁰ The magnetically dilute complexes give information about the couplings between lanthanoid centers. Besides its diamagnetic nature another of yttrium's benefits is that ^{89}Y is the only naturally occurring isotope of Y, which is beneficial in mass spectrometry.⁶

2.2. Cyclopentadienyls as ligands

Cyclopentadiene C_5H_6 as a neutral molecule is a five membered carbon ring that has formally two double bonds. Upon removing one proton a negative cyclopentadienyl anion $[C_5H_5]^-$ (Cp) can be generated from the cyclopentadiene framework. In cyclopentadienyl anion the π -electrons of two double bonds are conjugated between all five carbons creating a π -electron cloud that is delocalized through the whole molecule (Fig. 1).

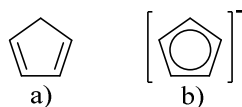


Figure 1. 1,3-cyclopentadiene (**1**) presented as a) neutral molecule with double bonds b) negatively charged cyclopentadienyl presented with the delocalization curve.

The delocalization of π -electrons is very important feature in the case of lanthanoid complexes of Cp- ligands. The importance is because Cp- ligands coordinate to lanthanoid center via delocalized π -cloud. One of the simplest complexes including lanthanoids and Cp- ligands are MCp_3 - complexes. The MCp_3 - complexes have one trivalent lanthanoid center ion and three Cp- ligands coordinated to center lanthanoid with their delocalized π -electrons. MCp_3 can be synthesized for all lanthanoids and Y by refluxing MCl_3 and NaCp in THF (Fig. 2).

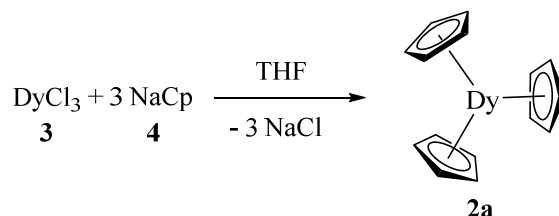


Figure 2. Reaction route for Dy^{3+} - complex **2a** ($DyCp_3$).^{1,11}

Because of delocalization of coordinating π -electrons Cp- ligands are generally presented as η^5 - ligands in lanthanoid complexes. η^5 - ligand means, that each Cp- ligand is coordinated to lanthanoid center formally with all five carbons. Categorizing Cp- ligands in lanthanoid complexes as η^5 -ligands emphasizes the perpendicular position of each Cp- ring against the coordination bond between center of Cp- ring and lanthanoid center (M-Cnt bond).

Orientations of simple Cp- ligands around oblate Dy^{3+} ion in complex **2a** are not ideal for high magnetic anisotropy and SMM behavior to develop. Fortunately, Cp- ligands can be modified with various functional groups. Such modified Cp- ligands include for example Cp^{Me} , Cp^{Me_4} , Cp^* , Cp^{SiMe_3} , $Cp^{(SiMe_3)_2}$, Cp^{tnt} and Cp^{iPr_5} that all are bulkier versions of Cp. In lanthanoid complexes with lanthanoid metallocenium unit $[MCp_2]^+$ use of bulkier Cp- ligands

like Cp^{iPr5} results in wider Cp-M-Cp bond angle, which is favorable thing in for example dysprosium SMMs. In addition to achieving good magnetic properties, Cp- ligands with different sizes are also used to stabilize otherwise reactive systems like divalent lanthanoid ions. In some cases, syntheses with differently sized lanthanoids require different Cp- ligands to work.

2.3. Basics of lanthanoid single molecular magnets

Single molecular magnets (SMM) are molecular species that show the slow relaxation of magnetization in low temperatures. The definition of SMM also includes that the magnetic properties of SMM are purely of molecular origin in contrast to classic bulk ferromagnets in which magnetic properties originates from interactions between magnetic domains. There are few physical quantities that are used to measure and determine qualities of SMMs. Most used quantities are the magnetic blocking temperature (T_b) and the magnetic anisotropy barrier (U_{eff}). T_b is the highest temperature where a magnetic hysteresis loop can be observed. In the magnetic hysteresis loop the magnetization M is plotted against the external magnetic field H in different temperatures below T_b . Another definition for T_b is a temperature, where a zero-field cooled and a field cooled magnetic susceptibilities coincides. Value of T_b depends slightly on the method used to determine it but also on the instruments used. Therefore, a standardized 100 s T_b (T_{b100}) is also used. T_{b100} is a temperature, where magnetic relaxation time is exactly 100 s.¹²

U_{eff} is an energy barrier between the lowest magnetic states of an SMM. In SMMs the lowest magnetic states are split in two states with opposite magnetic moments. Optimally all split states form a barrier between the two lowest states with opposite magnetic moments. This barrier is called U_{eff} . Without external magnetic field the populations of the two lowest states are in equilibrium. As the external magnetic field is applied along the direction of one of the SMMs lowest magnetic states, it causes the state with magnetic moment opposite to external magnetic field to have lower energy. Sudden energy difference between the two lowest states causes the population to switch mainly to state with magnetic moment opposite to external magnetic field. At this point, the SMM is magnetized.¹²

Slow relaxation of magnetization takes place when the external magnetic field is switched off. The system will now go back to the original equilibrium, but the slow relaxation of magnetization depends on the process through which the relaxation happens. Quantum tunneling of magnetization (QTM) is a rapid relaxation process that is very common for

lanthanoid complexes. QTM causes magnetization to transfer directly between the two lowest states and QTM must be quenched or at least suppressed for the slow relaxation of magnetization to be observed. The optimal slow relaxation of magnetization would take place over the full barrier, but especially for Ln-SMMs the relaxation happens usually between the few lowest states via thermally assisted processes called Raman- and Orbach processes and suppressed, but still existing, QTM. With these processes the relaxation usually occurs with energies much lower than U_{eff} is, which is why especially in Ln-SMMs T_b is much lower than U_{eff} .¹²

There are three important things to consider when choosing lanthanoid and ligands for new Ln-SMMs. First thing is magnetic moment of the lanthanoid ion. The magnetic moments of lanthanoid ions arise from the degenerated nature of 4f- orbitals. Unpaired electrons on well degenerated 4f- orbitals generate orbital angular momentum (L) that is strongly coupled with the total spin (S) of the system. The strong coupling between L and S results in the spin-orbit coupling ($J = L + S$) that largely determines the magnitudes of the effective magnetic moments of lanthanoid ions. Especially Dy^{3+} and Tb^{3+} have large magnetic moments due to many unpaired electrons on their 4f- orbitals. High magnetic moment of lanthanoid center of complex affects T_b and U_{eff} of the whole complex, but it alone does not guarantee suppressed QTM and SMM behavior.

Second thing is the magnetic anisotropy of complex. Lanthanoid ions used for Ln-SMMs must be magnetically anisotropic. The magnetic anisotropy on Ln-SMMs means that the magnetic moment of lanthanoid ion to aligns to the certain direction, that is, the easy axis of magnetization of the molecule. The magnetic anisotropy of lanthanoid complexes is caused by interactions between a lanthanoid ion and crystal field. The shape of electron density around lanthanoid ions is a crucial thing for favorable metal-ligand interactions and for the strength and axially of magnetic anisotropy of lanthanoid ion. M^{3+} lanthanoid ions appear in three different shapes that are oblate (equatorial spheroid), prolate (axial spheroid) and isotropic sphere. The shapes arise from occupations of differently aligned 4f- orbitals. Gd^{3+} -ion has one electron on each 4f- orbital and Lu^{3+} -ion has full 4f- orbitals so they are isotropic spheres. Pm^{3+} , Sm^{3+} , Er^{3+} , Tm^{3+} and Yb^{3+} -ions are prolate shaped, because of higher occupancy on axially oriented 4f- orbitals ($m_l = \pm 1$ or 0). Ce^{3+} , Pr^{3+} , Nd^{3+} , Tb^{3+} , Dy^{3+} and Ho^{3+} -ions are oblate shaped, because of higher occupancy on equatorially oriented 4f- orbitals ($m_l = \pm 3$). High single ion anisotropy can be achieved for prolate ions with the strong equatorial and weak axial ligand field and for oblate ions with strong axial and weak

equatorial ligand field. The strong axial anisotropy is important in Ln-SMMs, because it quenches the QTM relaxation process.¹³

Third essential thing for Ln-SMMs is bistability of the electronic ground state of lanthanoid ion. Correctly oriented ligand field is important also for the bistability. For complexes of M^{3+} -lanthanoid ions with even number of unpaired electrons, like Tb^{3+} , the bistable state can be achieved with the perfectly oriented coordination environment. Lanthanoid ions with uneven number of unpaired electrons like Dy^{3+} are Kramer's ions. Kramer's ions have bistable electronic ground state irrespective of their coordination environment, which means that the ligand field of Kramer's ion does not have to be perfectly oriented for complex to be an Ln-SMM. Cyclopentadienyl ligands are not usually oriented perfectly axially or perfectly equatorially, especially in lanthanoid metallocenium cations $[MCp_2]^+$, which is why Kramer's ions like Dy^{3+} show SMM properties even without perfect symmetry around coordination environment.^{10,13}

In most of the reported complexes, lanthanoid ions do not reside in the perfect coordination environment that would fully quench the QTM. This holds especially for multinuclear Ln-SMMs, that have more than one lanthanoid centers in the structure; it is harder to control the geometry around lanthanoid ions in multinuclear complexes than in mononuclear complexes. In multinuclear complexes, the QTM can be quenched by strong exchange coupling between the paramagnetic centers of system. For example, in lanthanoid complex with two paramagnetic Dy^{3+} centers and a bridging organic radical ligand between them, the equatorial ligand field generated by bridging ligand is unfavorable for strong axial anisotropy of oblate Dy^{3+} centers. However, the unpaired electron on radical bridging ligand may form exchange coupling with both Dy^{3+} centers. If the exchange coupling is strong enough, it will quench the QTM relaxation process.

3. Lanthanoid complexes with cyclopentadienyl ligands

3.1. Divalent mononuclear complexes

Divalent lanthanoid complexes are molecular species in which the formal oxidation state of lanthanoid ion is 2+. The divalent complexes have gained increasing interest during previous decade as they are not only potential building blocks for developing SMMs with higher T_b and U_{eff} , but they also provide general information about the fundamental properties of lanthanoids. Such fundamental properties are for example the reduction potentials of divalent lanthanoid complexes, ionic radii of M^{2+} ions in complexes and, the most importantly, electronic configurations of divalent lanthanoid ions in complexes. The determination of the electronic configurations has been a huge challenge. In this chapter the syntheses of divalent lanthanoid complexes as well as the main steps taken to determine their electronic configurations are discussed.

3.1.1. Synthesis of the whole series

The first organometallic divalent lanthanoid complexes EuCp_2 and YbCp_2 were synthesized in 1965 using liquid ammonia as a solvent.¹⁴ More lanthanoids were not added to the series of divalent complexes until during last ten years^{15,16} and the whole series was completed as late as in 2013.¹⁷ The progress in the discovery of divalent lanthanoid complexes was relatively slow because M^{2+} ions are highly reactive and synthesized complexes have been too instable to be examined. The first big step after 1965 was the synthesis of complexes **6a** and **6b** in 2008 (Fig. 3).

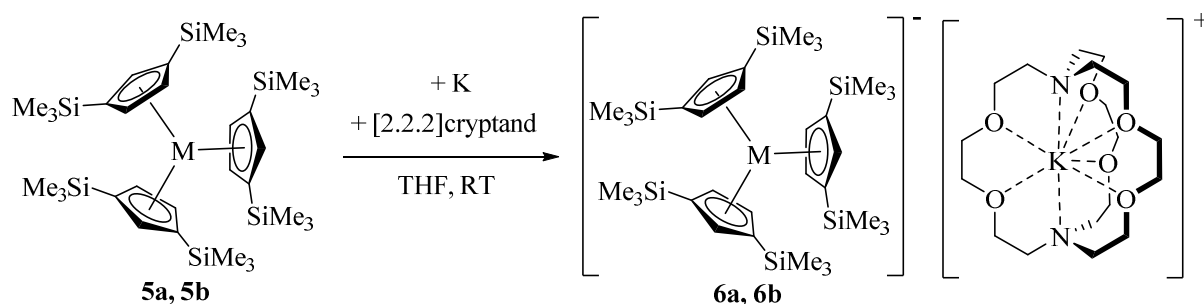


Figure 3. Reaction route for the complexes $[\text{K}(2.2.2\text{-Cryptand})][\eta^5\text{-Cp}^{(\text{SiMe}_3)_2}_3\text{M}]$, where $M = \text{La}^{2+}$ (**6a**) or Ce^{2+} (**6b**).¹⁶

Syntheses of **6a** and **6b** were also done with 18-crown-6 and metallic potassium. The synthetic route led to the mixture of compounds from which **6a** and **6b** could not be isolated. In contrast to 18-crown-6 and metallic potassium, [2.2.2]Cryptand and metallic potassium

worked in the room temperature and **6a** and **6b** were produced, isolated and defined to be divalent lanthanoid complexes.¹⁵

After synthesis of complexes **6a** and **6b** it took four years until the next set of divalent lanthanoid complexes were published. Before that, divalent yttrium complex $[\text{K}(18\text{-C-}6)][\eta^5\text{-Cp}^{\text{SiMe}_3}_3\text{Y}]$ was synthesized in 2011 using 18-crown-6 and metallic potassium.⁹ The lanthanum and cerium complexes **6a** and **6b** had been isolated with $\text{Cp}^{(\text{SiMe}_3)_2}$ - ligands, but they appeared to be too bulky to form complex with smaller yttrium. $\text{Cp}^{\text{SiMe}_3}$ - ligand was used instead of $\text{Cp}^{(\text{SiMe}_3)_2}$ - ligand and the synthesis worked in $-45\text{ }^\circ\text{C}$. Same $\text{Cp}^{\text{SiMe}_3}$ - ligand was also used in synthesis of **8a – 8e** in 2012 (Fig 4).¹⁵

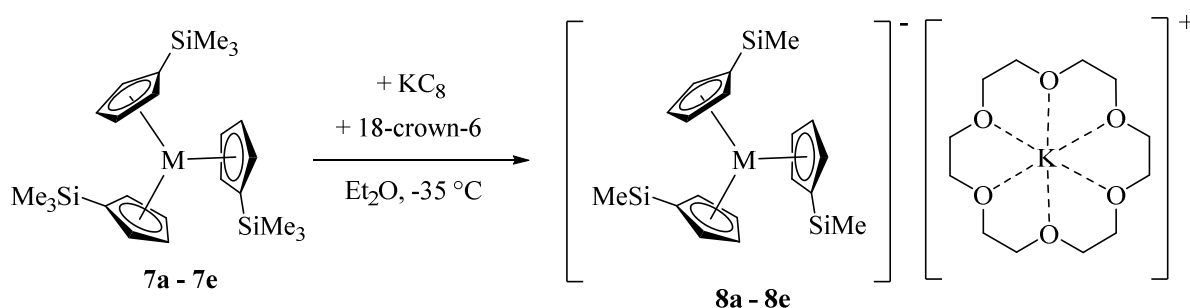


Figure 4. Reaction route for the complexes $[\text{K}(18\text{-C-}6)][\eta^5\text{-Cp}^{\text{SiMe}_3}_3\text{M}]$, where $\text{M} = \text{Pr}^{2+}$ (**8a**), Gd^{2+} (**8b**), Ho^{2+} (**8c**), Er^{2+} (**8d**) or Lu^{2+} (**8e**).^{15,17}

Complexes **8a - 8e** are reported to be air- and moisture sensitive like their corresponding trivalent complexes. In developing and optimizing the reaction route presented in Figure 4, the most important factors were the right type of ligands, precooling the solvent and glassware to $-35\text{ }^\circ\text{C}$, use of KC_8 instead of metallic potassium and employing diethyl ether as a solvent. KC_8 is a graphite intercalation compound and it is a powerful and fast reducing agent, more reactive than metallic potassium. The fast reduction was beneficial in the reaction because the temperature of the used glassware needed to stay below $-35\text{ }^\circ\text{C}$. Longer reaction time could have led the warming of the glassware and decomposition of the product. The choice of solvent is always an important factor in the synthesis and in the synthesis of **8a - 8e** it was crucial. The products **8a - 8e** decompose in THF, benzene and toluene and they also react with N_2 , which is why reactions had to be performed under an argon atmosphere. The cationic complex $[\text{K}(18\text{-C-}6)]^+$ formed from K^+ and chelating 18-crown-6 acts as a stabilizing counter cation for the anionic divalent lanthanoid complexes **8a - 8e**. The required specific reaction conditions in the synthesis of **8a - 8e** indicate the instability of divalent lanthanoid complexes towards ambient conditions.¹⁵

The series of M^{2+} -complexes was finally completed when the remaining complexes **9a - 9d** were synthesized and isolated in 2013 (Fig. 5).¹⁷

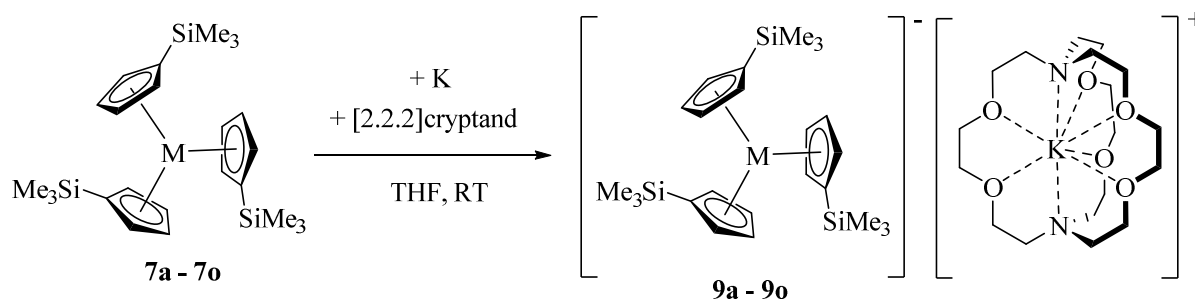


Figure 5. Reaction route for the complexes $[K(2.2.2\text{-Cryptand})][\eta^5\text{-Cp}^{\text{SiMe}_3}_3\text{M}]$, where $M = \text{Pr}^{2+}$ (**9a**), Gd^{2+} (**9b**), Tb^{2+} (**9c**), Lu^{2+} (**9d**), La^{2+} (**9e**), Ce^{2+} (**9f**), Nd^{2+} (**9g**), Sm^{2+} (**9h**), Eu^{2+} (**9i**), Dy^{2+} (**9j**), Ho^{2+} (**9k**), Er^{2+} (**9l**), Tm^{2+} (**9m**), Yb^{2+} (**9n**) or Y^{2+} (**9o**).¹⁷

Metallic potassium and [2.2.2]Cryptand were used instead of KC_8 and 18-crown-6 that were used for **8a - 8e**. The use of [2.2.2]Cryptand as a chelating agent for potassium ions allowed researchers to perform the synthesis at room temperature instead of at $-35\text{ }^\circ\text{C}$. After the isolation and characterization of **9a - 9d** the series of divalent $[\text{Cp}^{\text{SiMe}_3}_3\text{M}]^-$ complexes was finally completed. The $[\text{Cp}^{\text{SiMe}_3}_3\text{M}]^-$ parts of complexes **8a - 8e** and **9a - 9d** were comparative, but counter cations were still different, not to mention the complexes of six traditional divalent lanthanoids (Eu, Yb, Sm, Tm, Dy and Nd) that had been isolated merely as lanthanoid dihalides.¹⁷

3.1.2. Determination of electronic configurations

The major issue with the new complexes **6a**, **6b**, **8a - 8e** and **9a - 9d** was the differences in distances between the lanthanoid centers and centroids of cyclopentadienyl rings (M-Cnt). The M-Cnt distances in divalent complexes compared to the M-Cnt distances in their trivalent analogues were supposed to differ considerably because the M-X bond lengths ($M = \text{Eu, Yb, Sm, Tm, Dy or Nd}$, $X = \text{F}$ (for only Eu, Yb and Sm), Cl, Br or I)¹⁸ between the divalent and trivalent traditional lanthanoid halides differ roughly $0.10 - 0.20\text{ \AA}$. However, in the new complexes the differences in M-Cnt distances between divalent and trivalent complexes were only $0.020 - 0.032\text{ \AA}$. The new divalent complexes differed so little in M-Cnt distances from their trivalent analogues that it was questioned if the lanthanoid ions were divalent. One possible explanation for the observation was that lanthanoids in the new complexes had different electronic configuration than in the traditional compounds. The traditional divalent lanthanoids were defined to have $4f^{n+1}$ electronic configuration and their trivalent analogues $4f^n$ electronic configuration. There are clear differences in ionic radii between $4f^{n+1}$ and $4f^n$ configurations, because of constant contraction of 4f- orbitals. The differences in ionic radii

between $4f^n$ and $4f^n5d^1$ electronic configurations are not as large, because electron on 5d-orbital does not increase the size of ion as much as electron on 4f-orbital. Next step was to determine the configurations of lanthanoid centers in the new complexes to be sure, if all divalent lanthanoids had really been isolated as molecular species.⁷

To determine electronic configurations unambiguously, the whole series of complexes **9a** – **9o** (Fig. 5.) were synthesized for yttrium and all lanthanoids, except for promethium due to its radioactivity. The differences in M-Cnt distances between those new M^{2+} - complexes and their already known analogous M^{3+} - complexes were in different scale for some of the lanthanoids. Complexes of Eu, Yb, Sm, and Tm had larger differences (0.123–0.156 Å) in M-Cnt distances between the divalent and trivalent analogues and their M^{2+} - ions were concluded to possess $4f^{n+1}$ electronic configuration as defined before. Other examined lanthanoids (La, Ce, Pr, Gd, Tb, Ho, Er, and Lu) as well as yttrium had smaller differences in M-Cnt distances (0.020–0.032 Å) between divalent and trivalent analogues and their M^{2+} - ions were concluded to possess $4f^n5d^1$ electronic configuration. Differences in M-Cnt distances with Dy and Nd complexes suggested that their M^{2+} - ions were also obeying $4f^n5d^1$ electronic configuration and not the $4f^{n+1}$ configuration that had previously been determined for Dy^{2+} and Nd^{2+} in a different ligand field. This means that at least Dy^{2+} and Nd^{2+} can adopt either of the two different electronic configurations depending on the ligand field.⁷

M^{2+} - ion with $4f^n5d^1$ configuration could be a good thing in designing Ln-SMMs. The additional unpaired electron on 5d-orbital would lead to increased spin-orbit coupling, which would increase the magnetic moment of the lanthanoid ion. Therefore, magnetic properties of the M^{2+} complexes analogous to **9a** – **9o** and M^{3+} complexes were measured and examined for all lanthanoids, except for Pm, Yb and Lu. Pm was not examined because of its radioactivity and Yb and Lu were not examined because Yb^{2+} and Lu^{3+} both have fully occupied 4f-orbitals. The goal for the measurements was to examine if the magnetic moments of M^{2+} complexes agree with either $4f^{n+1}$ or $4f^n5d^1$ configurations that were previously determined using M-Cnt distances. Based on magnetic susceptibility measurements it was concluded that the electronic configurations of Sm^{2+} , Eu^{2+} and Tm^{2+} in the complexes were $4f^{n+1}$. Measured data for complexes of La^{2+} , Gd^{2+} , Tb^{2+} , Dy^{2+} , Ho^{2+} , Er^{2+} , Yb^{2+} , and Lu^{2+} as well as for Y^{2+} -complex suggested $4f^n5d^1$ - configuration. Electronic configurations for complexes of Ce^{2+} , Pr^{2+} and Nd^{2+} could not be determined unambiguously because measured data suggested electronic configuration somewhere in between those two possible configurations. The three divalent lanthanoids were thought to have mixed electronic configuration between $4f^{n+1}$ and $4f^n5d^1$. The mixed configurations cannot be determined by comparing the bond lengths of

analogous divalent and trivalent complexes. So, it was proven that Dy^{2+} and Nd^{2+} can switch between the two electronic configurations when coordination environment around lanthanoid center changes. Based on magnetic measurements Ce^{2+} , Pr^{2+} and Nd^{2+} ions seem to have mixed configurations in $[\text{K}(\text{2.2.2-Cryptand})][\eta^5\text{-Cp}^{\text{SiMe}_3}\text{M}]$ complexes. The structural and magnetic studies performed for complexes **9a** – **9o** outline that the divalent lanthanoids cannot be easily categorized to $4f^{n+1}$ or $4f^n5d^1$ configuration, because they may also switch between these configurations, when their coordination environment changes, or possess mixed configurations.^{7,19}

3.1.3 Other complexes of divalent lanthanoids

Divalent lanthanoid ions have been isolated also as other complexes than $\text{Cp}^{\text{SiMe}_3}\text{M}$. One different way to isolate M^{2+} ions with three conjugated ligands is the synthesis of $[(\text{MCp}^{\text{SiMe}_3})_2(\mu\text{-}\eta^6:\eta^6\text{-C}_6\text{H}_6)]^{2-}$ complexes for La^{2+} (**10a**) and Ce^{2+} (**10b**) (Fig. 6).²⁰

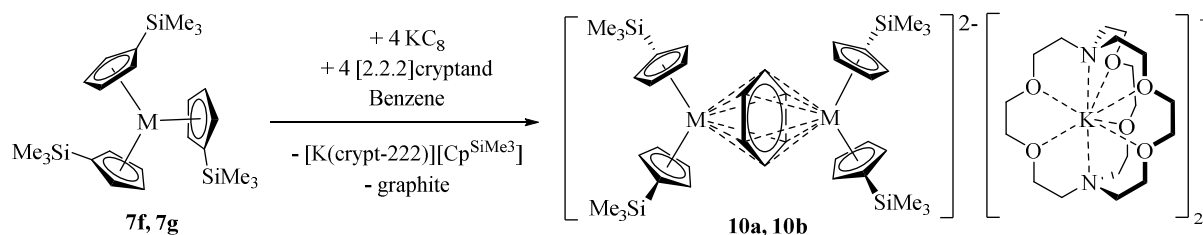


Figure 6. Reaction route for the complexes $[(\text{MCp}^{\text{SiMe}_3})_2(\mu\text{-}\eta^6:\eta^6\text{-C}_6\text{H}_6)]^{2-}$ where $\text{M} = \text{La}$ (**10a**) or Ce (**10b**).²⁰

This kind of reaction needs highly reductive conditions to happen, because benzene is difficult to reduce to $(\text{C}_6\text{H}_6)^{2-}$. Indeed, use of [2.2.2]Cryptand and KC_8 offer such reaction conditions and resulting $[\text{K}(\text{crypt-222})]^+$ cation helps stabilizing the products **10a** and **10b**. In products both M^{2+} ions were surrounded by three conjugated arene rings like in other divalent lanthanoid complexes **9a** – **9o**. Complexes **10a** and **10b** were the first complexes of divalent lanthanoids, where all arene ring ligands were not cyclopentadienyls.²⁰

Like in the complexes **9a** – **9o**, the problem with complexes **10a** and **10b** was to determine, if the lanthanoids really were divalent. Additional difficulty arose from the electronic structure of benzoate ligand that could be either $(\text{C}_6\text{H}_6)^{2-}$ or $(\text{C}_6\text{H}_6)^{4-}$. The presence of $(\text{C}_6\text{H}_6)^{2-}$ and $(\text{C}_6\text{H}_6)^{4-}$ would indicate divalent and trivalent lanthanoids, respectively. Methods used to determine the oxidation states of lanthanoid ions were magnetic measurements, structural analysis, UV/VIS spectrophotometry, DFT calculations and redox experiments. Magnetic measurements included ^1H NMR and magnetic susceptibility measurements, but they did not

offer information for or against the existence of divalent lanthanoids. Crystal structure of **10a** showed twisted C₆H₆- ring, which is indicative for (C₆H₆)²⁻.²⁰

UV/VIS- spectra of products **10a** and **10b** were similar shape to those of starting materials **7f** and **7g**, but with much higher extinction coefficients. Usually lanthanoid complexes like **7f** and **7g** have extinction coefficients of 1000 – 2000 M⁻¹ cm⁻¹ and their divalent analogues have extinction coefficients of 900 M⁻¹ cm⁻¹, but for **10a** and **10b** the coefficients were around 8000 M⁻¹ cm⁻¹. Reason for this could not be explained. DFT calculations performed for divalent [(MCp^{SiMe₃})₂(μ-η⁶:η⁶-C₆H₆)]²⁻ complex revealed that two highest occupied molecular orbitals HOMO and HOMO-1 have much more ligand character than those of trivalent complexes like **7f** and **7g** usually have. The calculations indicate that complexes **10a** and **10b** are divalent lanthanoids. UV/VIS spectrum was also simulated for computational [(MCp^{SiMe₃})₂(μ-η⁶:η⁶-C₆H₆)]²⁻ species and it appeared to be very similar to experimental spectra. In redox experiments complexes **10a** and **10b** reduced naphthalene by four electrons and 1,3,5,7-cyclooctatetraene by one electron, but they did not reduce N₂. The reactivity could be explained with existence of divalent lanthanoids, but on the other hand, complexes of trivalent lanthanoids would include (C₆H₆)⁴⁻ ligand that is also reactive and might be able to perform the same reductions.²⁰

By considering the carried-out measurements, calculations and redox experiments, complexes **10a** and **10b** were concluded to be the divalent lanthanoid complexes with bridging (C₆H₆)²⁻ ligand. Ligand character of HOMO- orbitals suggested that divalent lanthanoids could possibly be isolated with other arene rings than cyclopentadienyl and benzyl. Explaining the high extinction coefficients of UV/VIS spectra of **10a** and **10b** requires more research and isolation of novel divalent lanthanoids in different ligand fields.²⁰

3.2. Trivalent mononuclear complexes

Major development of Ln-SMMs started from the simple mononuclear complexes. In the late 2000s and in the early 2010s progression in the field of Ln-SMMs has been made on polynuclear bridged complexes, which are discussed later in this thesis. Lately focus has turned back to mononuclear complexes, which allow the symmetry of ligand field to be tuned in more controlled fashion. In this chapter synthetic methods involving [BPh₄]⁻ ligand are first introduced and then the magnetic capabilities of dysprosium metallocenium complexes are presented and discussed.

3.2.1. Synthetic capabilities of $[\text{Cp}^*_2\text{M}][\text{BPh}_4]$

One widely used weakly coordinating anion in the synthetic organometallic chemistry is $[\text{BPh}_4]^-$ that is also used as a ligand in $[\text{Cp}^*_2\text{M}][\text{BPh}_4]^-$ complexes. The complexes are used as precursors in synthetic chemistry because of their high reactivity and synthetic capabilities to make, for example, sterically crowded $\text{Cp}^*_2\text{M-R}$ complexes.²¹ The reactivity of $[\text{Cp}^*_2\text{M}][\text{BPh}_4]^-$ complexes rises from weak bonding interactions between $[\text{BPh}_4]^-$ and metal center. Typical and usually expected reaction of $[\text{Cp}^*_2\text{M}][\text{BPh}_4]^-$ complexes of lanthanoids is substitution of the $[\text{BPh}_4]^-$ ligand by oxygen or nitrogen containing ligands that coordinate strongly to oxophilic lanthanoid ions. This synthetic strategy was used at various syntheses, when the reactiveness of $[\text{Cp}^*_2\text{Sm}][\text{BPh}_4]$ (**11a**) was investigated (Fig. 7).²²

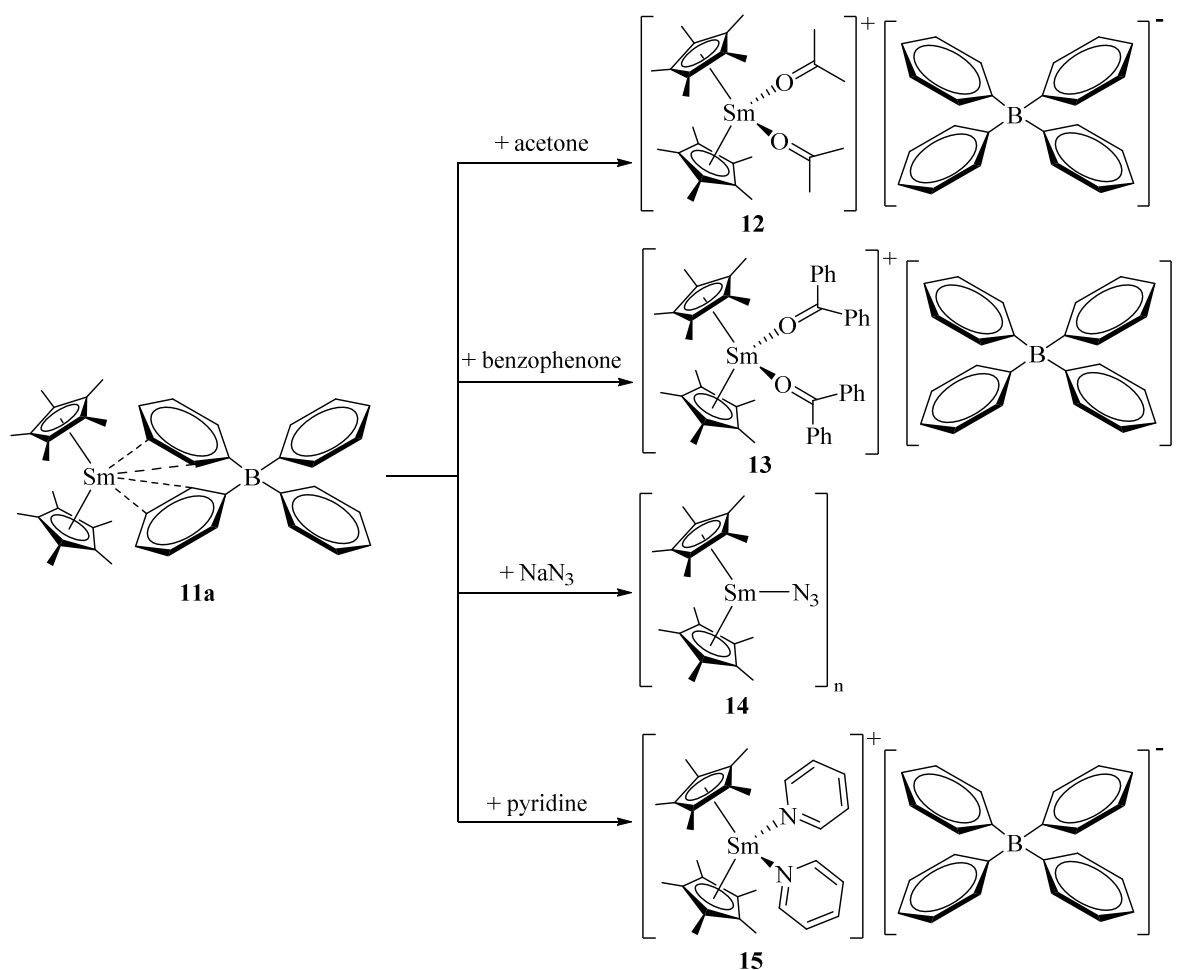


Figure 7. Reaction routes for complexes $[\text{Cp}^*_2\text{Sm}(\text{OCMe}_2)_2]^+$ (**12**), $[\text{Cp}^*_2\text{Sm}(\text{OCPh}_2)_2]^+$ (**13**), $[\text{Cp}^*_2\text{SmN}_3]_n$ (**14**) and $[\text{Cp}^*_2\text{Sm}(\text{py})_2]^+$ (**15**).²²

Reactions occurred as predicted and $[\text{BPh}_4]^-$ ligand was substituted by acetone, benzophenone, $[\text{N}_3]^-$ and pyridine to form **12**, **13**, **14** and **15** respectively. The products **12**, **13** and **15** are salts formed from cationic complex and $[\text{BPh}_4]^-$ counter anion, whereas the

product **14** crystallizes in two different crystal forms depending on crystallization conditions. The trimeric form of **14** crystallized from cold -30°C acetonitrile (MeCN) solution and polymeric form of **14** crystallized from hot MeCN solution of **14** when it was allowed cool to the room temperature. In both forms of complex **14** N_3^- ligands are bridging between Sm centers. This type of an end to end M-NNN-M bridging has been observed before in for example polynuclear terbium complex $[(\eta^3\text{-B}(\text{N}_2)_3)_2\text{Tb}(\mu\text{-N}_3)_4]$.^{22,23}

Synthetic chemistry is not always straightforward and predictable. Sometimes good results can be achieved albeit the original hypothesis is not fulfilled. Even with well-known synthetic routes reactions do not always occur as expected, or other unexpected reaction takes place. One of these cases was the intended synthesis of dysprosium complex **11b** $[\text{Cp}^*_2\text{Dy}][\text{BPh}_4]$ that had been successfully synthesized before, but the unexpected reaction occurred instead (Fig. 8).²⁴

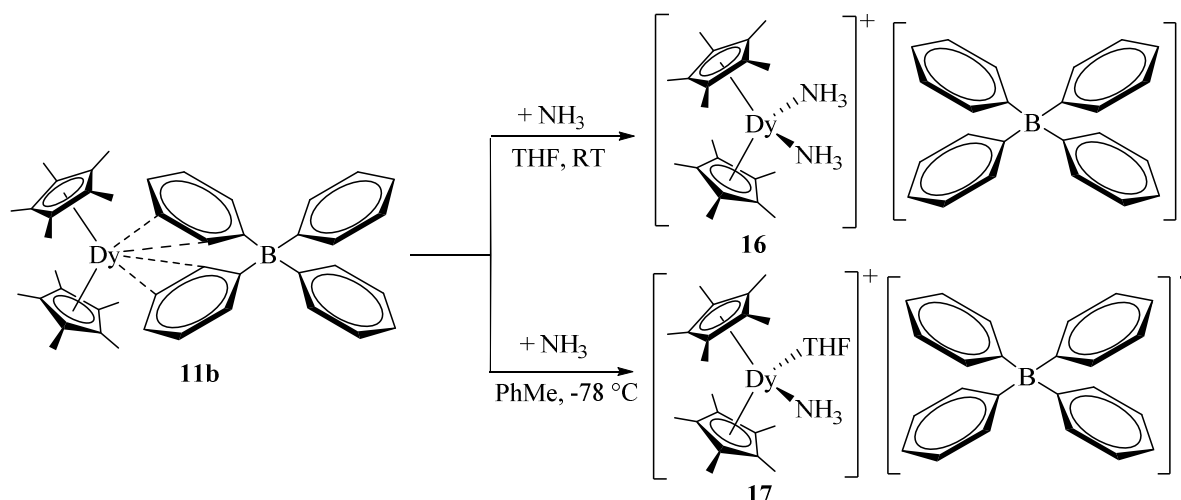


Figure 8. Reaction routes for the complexes $[\text{Cp}^*_2\text{Dy}(\text{NH}_3)_2][\text{BPh}_4]$ (**16**) and $[\text{Cp}^*_2\text{Dy}(\text{NH}_3)(\text{THF})][\text{BPh}_4]$ (**17**).²⁴

Researchers tried to synthesize more of the complex **11b** and managed to do it, but they also isolated the complex **16** from the reaction mixture. As discussed earlier, $[\text{BPh}_4]^-$ is a weakly coordinating anion that can easily be substituted with other ligands forming stronger coordination bonds to metal center than $[\text{BPh}_4]^-$. While working with weakly coordinating anions like $[\text{BPh}_4]^-$, special attention must be paid to the right reaction environment and solvent. For synthesis of **16**, finding the source of ammonia in the original reaction and optimizing the reaction conditions for producing **16** were pursued. Original source of ammonia could not be accurately determined, but researchers suspected ammonia to originate from NH_4Cl used in drying DyCl_3 , one of the starting materials of the complex **11b**. Reaction route for the complex **16** was optimized and complex **17**, the THF-adduct of the complex **16**,

was also isolated. Another serendipitous discovery was isolation of $\text{Cp}^*\text{Dy}(\text{C}_3\text{H}_5)_2(\text{THF})$ from reactions done to identify the source of ammonia. Crystal structures were determined for all three isolated complexes, but the complex **17** and $\text{Cp}^*\text{Dy}(\text{C}_3\text{H}_5)_2(\text{THF})$ were not examined further.²⁴

Magnetic measurements were performed for the complex **16** and it was determined to be an Ln-SMM with the magnetic anisotropy barrier of $U_{\text{eff}} = 546(6) \text{ cm}^{-1}$, which is more than 150 % larger than with the starting material **11b** ($U_{\text{eff}} = 339 \text{ cm}^{-1}$), that also showed the slow relaxation the magnetization. The improvement in U_{eff} was thought to be because NH_3 - groups are sterically less demanding than phenyl groups of $[\text{BPh}_4]^-$ ligand. Less bulky ligand caused Cnt-Dy-Cnt bond angle between centroids of Cp- ligands and Dy^{3+} in the complex **16** to be wider (140.2°) than corresponding bond angle in starting material **11b** (134.0°). Wider Cnt-Dy-Cnt bond angle causes a stronger axial coordination environment for Dy^{3+} center increasing the magnetic anisotropy and U_{eff} of the complex. The original goal of research was not achieved, but unexpected reaction offered other interesting results instead.²⁴

3.2.2. Low coordinated complexes

Dysprosium metallocenium complexes have provided to be the best Ln-SMMs so far. Such Ln-SMM is **19** that was exceptionally published by the two different research groups simultaneously. **19** has the magnetic blocking temperature of $T_b = 60 \text{ K}$. Anisotropy barriers were determined to be $U_{\text{eff}} = 1277 \text{ cm}^{-1}$ or $U_{\text{eff}} = 1223 \text{ cm}^{-1}$ by Guo *et al.* and Goodwin *et al.* respectively. (Fig. 9).^{2,3}

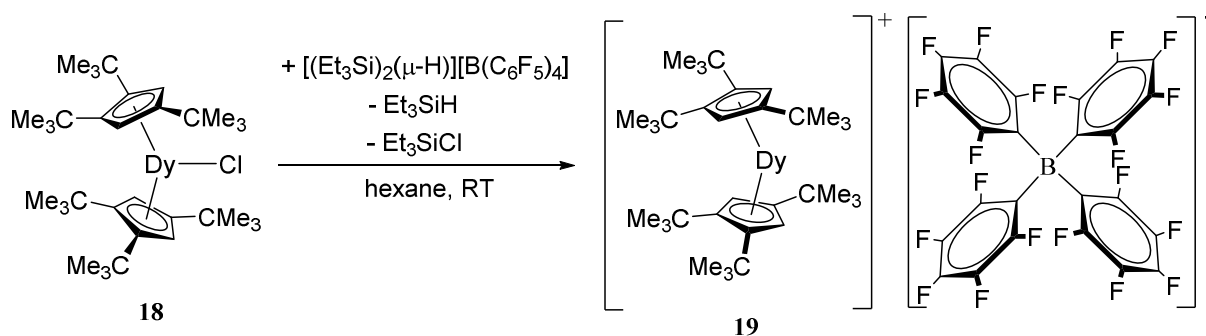


Figure 9. Reaction route for $[(\text{Cp}^{\text{ttt}})_2\text{Dy}][\text{B}(\text{C}_6\text{F}_5)_4]$ (**19**).^{2,3}

The complex **19** was synthesized from the complex **18** using a strong chlorine attractor and the resulting complex **19** was isolated as a cation with the non-coordinating anion $[\text{B}(\text{C}_6\text{F}_5)_4]^-$. In addition to its SMM properties complex **19** was remarkable discovery because it was the first lanthanoid metallocenium cation ever reported. The lanthanoid metallocenium cation is

the cationic complex with lanthanoid center being sandwiched by two cyclopentadienyl ligands. In **19** bulky Cp^{ttt}- ligands and bulky [B(C₆F₅)₄]⁻ counter cation are stabilizing otherwise reactive system that it can be isolated and examined. The absence of equatorial ligands and two axial Cp^{ttt}- ligands with the wide Cnt-Dy-Cnt bond angle (152.845(2)°) result in the strong axial and weak equatorial ligand field around Dy³⁺ centers which are the major factors causing the remarkable SMM properties of the complex **19**. Also Dy-Cp^{ttt} distances are only 2.324(1) Å and 2.309(1) Å that are quite short allowing even better metal-ligand interactions and the stronger axial ligand field.³

Records for properties of Ln-SMMs and SMMs were broken again in 2018. The record breaking Ln-SMM was complex **22** that has the magnetic anisotropy barrier of $U_{eff} = 1541 \text{ cm}^{-1}$ and blocking temperature of $T_b = 80 \text{ K}$. The blocking temperature of 80 K is significant, because it is above the temperature of 77 K where nitrogen liquefies. 77 K is thought to be the essential temperature barrier for developing usable nanomagnet devices (Fig. 10).⁴

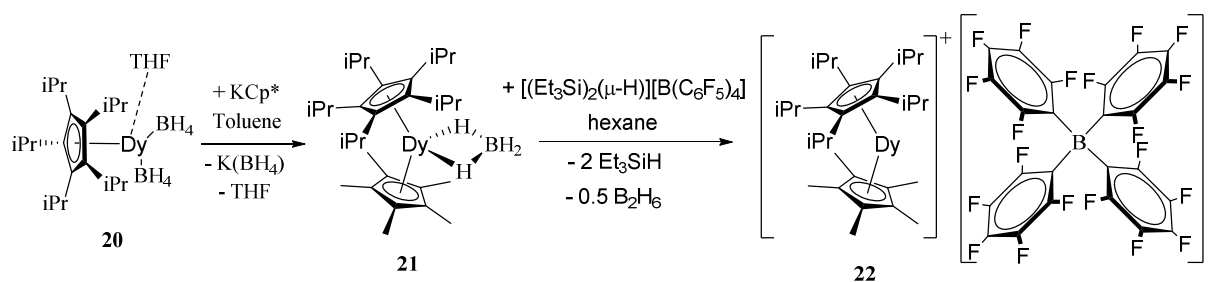


Figure 10. Reaction route for complex [(Cp^{iPr5})Dy(Cp*)][B(C₆F₅)₄] (**22**).⁴

The starting material of complex **22** had [BH₄]⁻ ligand instead of chlorine anions. Otherwise the step from hydride bridged complex **21** to low coordinated complex **22** follows the similar route as the synthesis of **19** with the same [B(C₆F₅)₄]⁻ counter anion. The high T_b and U_{eff} of complex **22** arise from good structural parameters that are the wide Cnt-Dy-Cnt bond angle and short bond lengths of Cp*-Dy and Cp^{iPr5}-Dy bonds. Cnt-Dy-Cnt bond angle in crystal structure of **22** was measured to be 162.507(1)°, which is 9.7° wider than the corresponding bond angle in complex **19**. Cp*-Dy and Cp^{iPr5}-Dy bond lengths in **22** were 2.296(1) Å and 2.284(1) Å respectively. The bond distances were on average 0.026 Å shorter than the corresponding bonds in complex **19**. The structural parameters explain why T_b and U_{eff} of complex **22** are even higher than those of complex **19**. The structural parameters and good magnetic properties of both complexes **19** and **22** make them excellent examples about benefits of mononuclear and low coordinated SMMs over polynuclear and high coordinated ones.⁴

3.3. Polynuclear heteroatom bridged complexes

3.3.1. N-bridged complexes

The N-bridged lanthanoid complexes refer to the complexes in which two or more lanthanoid centers are linked together with bridging ligands containing nitrogen atoms as hard donors. Typically, hard donor atoms are electron rich atoms with small atomic radii such as nitrogen and oxygen. The N-bridged lanthanoid complexes were mainly developed and investigated before 2010, but some recent discoveries have been also made with the radical N-bridging ligands.

Inspired by metal organic frameworks (MOFs) consisting of transition metals and various amines, dimeric complexes **24a – 24d** were synthesized in 2006. In the complexes lanthanoid centers are bridged with the organic amine groups acting as hard donors (Fig. 11).

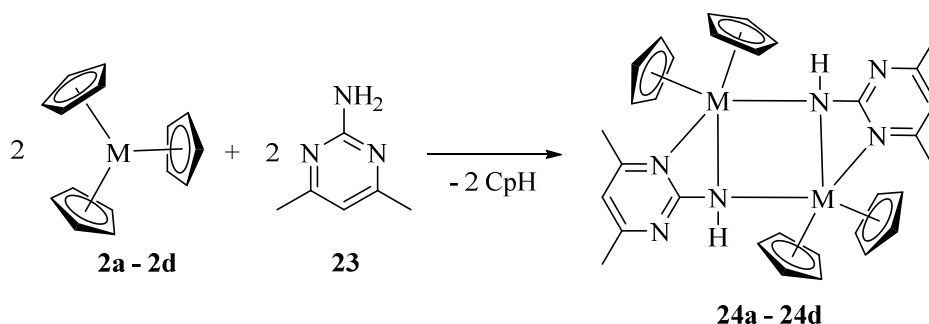


Figure 11. Reaction route for the complexes $[\text{Cp}_2\text{M}\{2\text{-NH-4,6-Me}_2\text{pm}\}]_2$ where M = Nd (**24a**), Gd (**24b**), Dy (**24c**) or Yb (**24d**).²⁵

The complexes **24a – 24d** were synthesized from the complexes **2a – 2d** with corresponding lanthanoids and the complex **23** (2-amino-4,6-dimethylpyrimidine) via the deprotonation of the amino group of **23**. This type of deprotonation reaction was already known, but it had not been applied to lanthanoid complexes before. Magnetic properties of the complexes were measured, but they were not SMMs. Formations of **24a – 24d** were more or less expected, but the surprising part of the study was formation of **26** (Fig. 12).²⁵

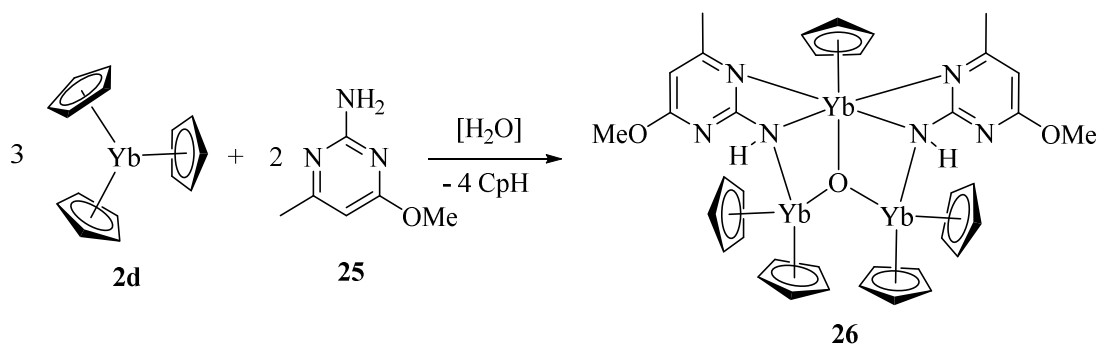


Figure 12. Reaction route for the complex $[\text{Cp}_2\text{Yb}(2\text{-NH-4-MeO-6-MeOpm})_2(\mu_3\text{-O})(\text{YbCp})]$ (**26**).²⁵

The complex **26** was synthesized from the complex **25**. The factor that led to the formation of the trinuclear complex **26** was the presence of water. Water was not added to the reaction mixture on purpose, but the reaction conditions were not entirely air- and moisture free. Usually lanthanoid complexes are synthesized in air- and moisture free environment, but not all lanthanoid complexes are that sensitive. Complex **26** is also not an SMM. Reactions presented in Fig. 11 and in Fig. 12 prove that it is possible to synthesize various polynuclear lanthanoid complexes through the direct metalation reactions between amines and tris cyclopentadienyl lanthanoid. The reactions open a way to future research for synthesizing new polynuclear lanthanoid-amino complexes with better catalytic and magnetic properties.²⁵

Reactions between MCp_3 and amines were studied further in 2010. In this study two complexes **24c** and **28** were synthesized to compare their properties to one another (Fig. 13).²⁶

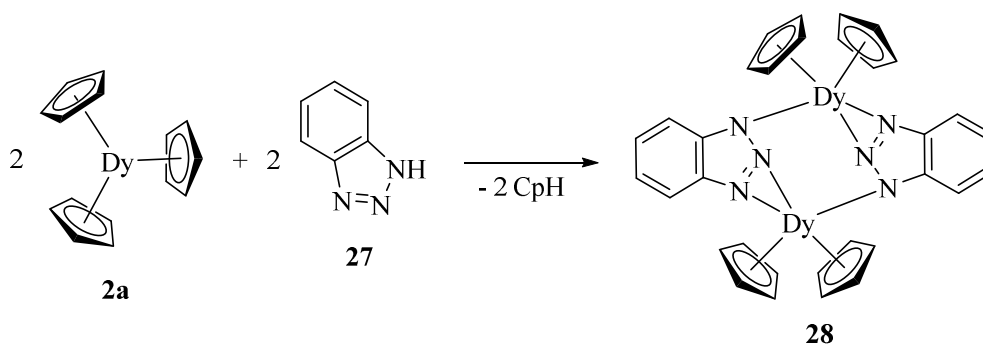


Figure 13. Reaction route for the complex $[\{\text{Cp}_2\text{Dy}(\mu\text{-bta})\}_2]$ (btaH=1H-1,2,3-benzotriazole) (**28**).²⁶

Reaction in Fig. 13 happened via the deprotonation of amino group of **27** like in the reactions presented in Fig. 11. In the complex **28**, benzotriazole ligand bridges two Dy^{3+} centers having all its three nitrogen atoms coordinated to Dy^{3+} ions. In the crystal structure of **28** equatorial benzotriazole ligands are in same plane with each other and Dy^{3+} ions. The crystal structure of the complex **24c** is twisted and none of the ligands are in the same plane.

Miscellaneous ligand field in **24c** does not support strong axial and weak equatorial ligand field that oblate Dy^{3+} - ions would require to show the strong magnetic anisotropy. The ligand field geometry of the complex **28** is more promising, because of axial Cp- ligands.²⁶

Magnetic properties of the complexes **24c** and **28** were compared by performing low temperature ac susceptibility measurements and DFT calculations. The complex **24c** did not show the slow relaxation of magnetization, but **28** did. Reason for this was clarified by DFT calculations. Exchange interaction was found between two Dy^{3+} - centers in **24c**, but not in **28**. The exchange interaction in the complex **24c** was too weak to have prominent influence on the static magnetic behavior. Therefore, the exchange interaction in **24c** could not be seen in experimental results. However, the exchange interaction between Dy^{3+} ions seems to be enough to provide the magnetic relaxation mechanism for the complex **24c**. The magnetic relaxation mechanism leads to fast relaxation of magnetism in **24c**, hence the magnetic behaviors of **24c** and **28** could not be compared and effects of different crystal fields could not be discussed. Nonetheless the complex **28** was a step closer to useful amine bridged Ln-SMMs and could be developed further.²⁶

One of the simplest N-bridging ligands are $\mu\text{-}\eta^2\text{:}\eta^2\text{-(N}_2\text{)}^{2-}$ and its radical form $\mu\text{-}\eta^2\text{:}\eta^2\text{-(N}_2\text{)}^{\bullet 3-}$. Complexes with $(\text{N}_2)^{2-}$ bridging ligand can be synthesized as shown in Fig. 14.²⁷

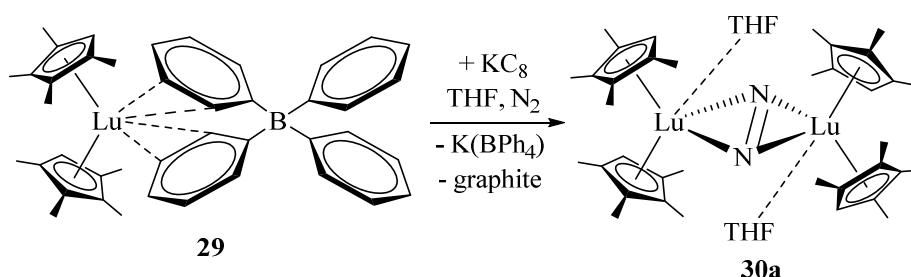


Figure 14. Reaction route for the complex $[(\text{Cp}^{\text{Me}4})_2(\text{THF})\text{Lu}]_2(\mu\text{-}\eta^2\text{:}\eta^2\text{-N}_2)$ (**30a**).²⁷

The complex **30a** was first synthesized from $(\text{Cp}^{\text{Me}4})_3\text{Lu}$ as its reactivity was studied. $(\text{Cp}^{\text{Me}4})_3\text{Lu}$ was synthesized with multistep reaction involving the complex **29**. The complex **29** was used in the synthesis of **30a** to skip the reaction steps that were needed to synthesize $(\text{Cp}^{\text{Me}4})_3\text{Lu}$. Nitrogen was present, because synthesis was carried out in air- and moisture free N_2 atmosphere using dry THF as solvent. In addition to the complex **30a** also $(\text{Cp}^{\text{Me}4})_3\text{Lu}$ was synthesized for the first time in 2005. $(\text{Cp}^{\text{Me}4})_3\text{Lu}$ was the last of $(\text{Cp}^{\text{Me}4})_3\text{M}$ complexes to be synthesized. N_2 is usually an inert gas, but the reactivity of the complex **29** and reducing power of KC_8 were enough to reduce N_2 to $(\text{N}_2)^{2-}$.²⁷

The dinitrogen bridged lanthanoid complexes can be refined into good Ln-SMMs, as will be discussed later, but they also provide valuable information about the chemistry of lanthanoid

complexes. A good example of this kind of research was synthesis of **32** and **34a-c** (Fig. 15).²⁸

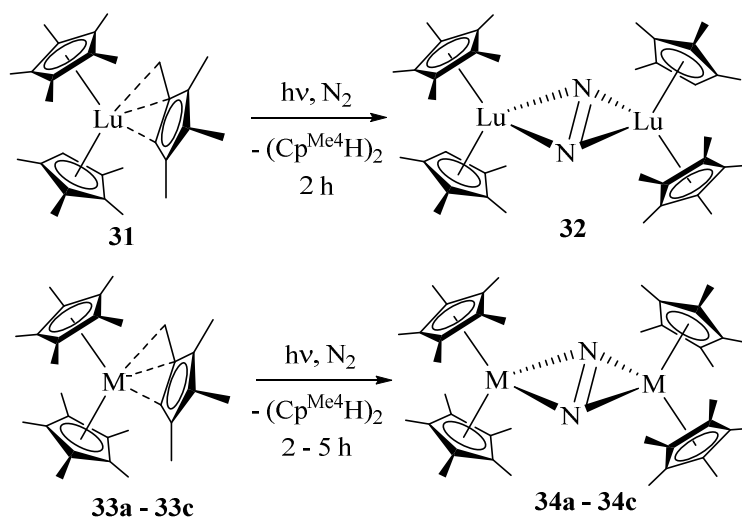


Figure 15. Reaction routes for complexes $[Cp^*Cp^{Me4}Lu]_2(\mu-\eta^2:\eta^2-N_2)$ (**32**) and $[(Cp^*)_2M]_2(\mu-\eta^2:\eta^2-N_2)$, where $M = Y$ (**34a**), Lu (**34b**) or Dy (**34c**).²⁸

Reactions in Fig. 15 were done with the photochemical activation instead of with generally used potassium reagents. First, complexes **31** and **33a** were left to the room temperature under air- and moisture free N_2 atmosphere for 3 weeks. Syntheses of **32** and **34a – 34c** were done irradiating NMR-scale samples with the mercury vapor lamp. Irradiation caused reaction times to drop from 3 weeks to 2 – 5 hours. Explanation for the unexpected reactivity was found from the crystal structures of heteroleptic starting materials **31** and **33a – 33c**. In the crystal structures of complexes **31** and **33a – 33c** one of the Cp^{Me4} - ligands in each complex is coordinated to metal center in different way than two other cyclopentadienyl ligands. These differently coordinated Cp^{Me4} - ligands are the ones that are substituted by dinitrogen bridging ligands in reactions.

The UV/VIS- spectra of starting materials **31** and **33a – 33c** were measured and compared to the UV/VIS- spectra measured from their corresponding homoleptic Cp^{Me4}_3M complexes. The complexes **31** and **33a – 33c** each produce two different absorptions, but their homoleptic analogues produce only one absorption each. The extra absorptions arise from the differently coordinated Cp^{Me4} - ligands. The DFT calculations showed that the HOMOs of the starting materials **31** and **33a – 33c** were mainly localized on the differently coordinated Cp^{Me4} - ligands, when the HOMOs of homoleptic complexes $(Cp^{Me4})_3M$ with corresponding metal centers were localized evenly on all three Cp^{Me4} - ligands. This suggests the weaker coordination bond between the ligand and M^{3+} - ion, thus it increases the reactivity of the differently coordinated Cp^{Me4} - ligand. Based on the results, lanthanoids cyclopentadienyl

complexes can be reactive enough to reduce the inert N_2 gas. It was recommended that UV/VIS- spectra would be measured from all new lanthanoids cyclopentadienyl complexes from now on so that their possibly special photochemical properties would be found and characterized.²⁸

The $(N_2)^{2-}$ - bridged complexes have been developed further by reducing the bridging $\mu\text{-}\eta^2\text{:}\eta^2\text{-}(N_2)^{2-}$ ligand to the radical $\mu\text{-}\eta^2\text{:}\eta^2\text{-}(N_2)^{\cdot-}$. The complexes with the neutral $(N_2)^{2-}$ - bridging ligand and Gd (**30b**), Tb (**30c**) or Dy (**30d**) as M^{3+} - center ion were synthesized according to reaction route in Fig. 14. The complexes were then reduced to the radical $\mu\text{-}\eta^2\text{:}\eta^2\text{-}(N_2)^{\cdot-}$ - bridged complexes **35a – 35c** that were used in synthesis of **36a** and **36b** (Fig. 16).²⁹

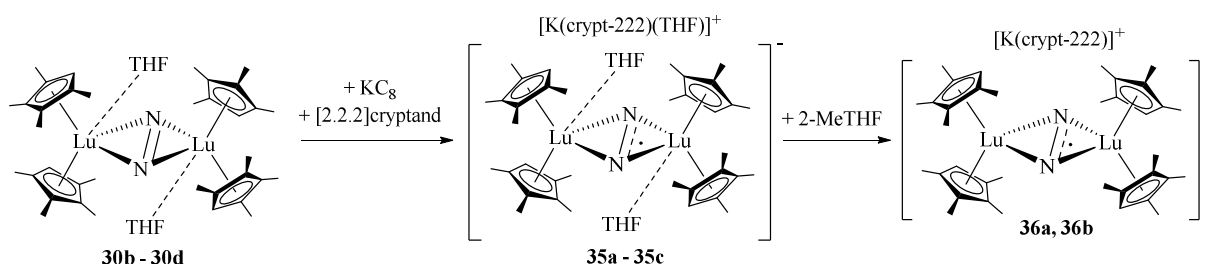


Figure 16. Reaction routes for the radical complexes

$[(Cp^{Me^4})_2M(THF)_2(\mu\text{-}\eta^2\text{:}\eta^2\text{-}N_2^{\cdot-})]^-$, where M = Gd (**35a**), Tb (**35b**) or Dy (**35c**)

and $[(Cp^{Me^4})_2M]_2(\mu\text{-}\eta^2\text{:}\eta^2\text{-}N_2^{\cdot-})]^-$, where M = Tb (**36a**) or Dy (**36b**).²⁹

The aim of the research was to synthesize low coordinated Ln-SMMs with the paramagnetic bridging ligand that would promote the direct exchange coupling between the unpaired electron of radical ligand and spins of lanthanoid ions. The strong enough direct exchange coupling quenches the QTM relaxation process and improves the overall magnetic properties of complexes. Cp^{Me^4} was chosen for the ligand because it was already used in synthesis of complex **30a** and as a bulky Cp- ligand it provides a wider Cnt-Dy-Cnt bond angle that enhances the magnetic anisotropy of oblate M^{3+} ions within the complexes **36a** and **36b**.²⁹

The hypothesis appeared to be right. The complex **36a** was reported to have the two magnetic anisotropy barriers with $U_{eff\ 1} = 276\text{ cm}^{-1}$ and $U_{eff\ 2} = 564\text{ cm}^{-1}$. The 100-s blocking temperature for complex **36a** was $T_b = 20\text{ K}$. Also, exchange coupling constant for Gd³⁺ complex **35a** was quantified to be $J = -20\text{ cm}^{-1}$, which refers to the strong antiferromagnetic coupling between the unpaired electron of radical ligand and Gd³⁺ ions. Likewise complexes **35b**, **35c**, **36a** and **36b** were concluded to also have the strong antiferromagnetic exchange couplings. U_{eff} and T_b of **36a** were records for the exchange coupled SMMs at the time of research and exchange coupling constant J of **35a** was the second largest observed for the Gd-complexes. Although the exchange coupling constants were not accurately determined for Tb-

and Dy- complexes **35b**, **35c**, **36a** and **36b**, the magnetic susceptibility data indicated the strong exchange couplings between the radical bridging ligands and lanthanoid centers also in the Tb- and Dy- complexes. U_{eff} and T_b of **36a** are nowhere near the ones that were measured by Guo *et al.*⁴ from their $[(Cp^{iPr5})Dy(Cp^*)]^+$ complex, but complexes **36a** and **36b** are still remarkable discoveries in the field of single molecular magnetism.²⁹

The radical N-bridged complexes have also been made with the organic redox active bridging ligands like 2,2'-bipyrimidinyl- (bpym), 2,3,5,6-tetra(2-pyridyl)pyrazinyl (tppz) and indigo. The radical bpym \cdot ligand was used as the N-bridging ligand in complexes **37a** – **37c** in 2012 (Fig. 17).³⁰

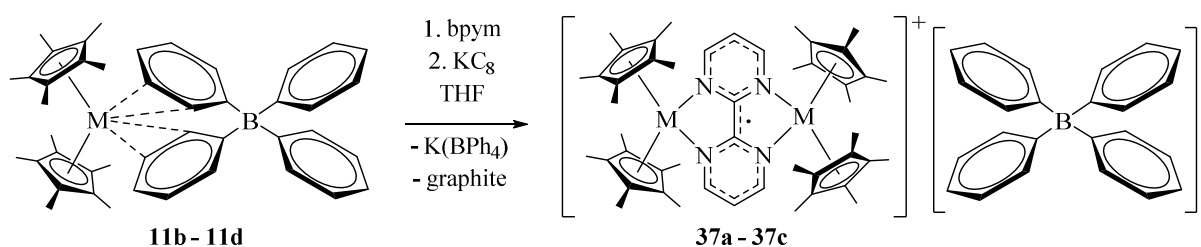


Figure 17. Reaction route for the complexes $[(Cp^*_2M)_2(\mu-\eta^2:\eta^2-bpym\cdot)] [BPh_4]$, where M = Gd (**37a**), Tb (**37b**) or Dy (**37c**).³⁰

The synthesis of complexes **37a** – **37c** worked as expected. First the bpym was added to the reaction solution to allow the neutral complexes to form and then KC_8 was added to the solution to reduce bpym- ligand to its radical form. The complexes **37a** – **37c** were synthesized, because the radical bridged complexes show great potential to be good Ln-SMMs as discussed above. Moreover, the use of the conjugated organic nitrogen containing bridging ligand, bpym, provides synthetic controllability over the N_2 bridging ligand. The delocalization of unpaired electron over the whole molecular framework in bpym increases its stability compared to bridging radical $(N_2)^{2-}$ - ligand. Organic conjugated ligands may also be reduced more than once allowing the tuning of magnetic exchange couplings between the radical bridging ligand and lanthanoid centers without changing ancillary cyclopentadienyl ligands.³⁰

The magnetic properties of **37a** – **37c** were measured and intramolecular Gd^{3+} -bpym \cdot exchange coupling constant for **37a** was determined to be $J = -10 \text{ cm}^{-1}$, which means a strong antiferromagnetic coupling between unpaired electrons of the radical bpym \cdot ligand and Gd^{3+} ions. Also, **37b** and **37c** were concluded to have antiferromagnetic M^{3+} -bpym \cdot exchange couplings. **37b** and **37c** are also SMMs with the magnetic anisotropy barriers of $U_{eff} = 44 \text{ cm}^{-1}$ and $U_{eff} = 87.8 \text{ cm}^{-1}$ respectively. These numbers were remarkable for radical bridged multinuclear lanthanoid complexes in 2012.³⁰

Ln-SMMs with organic radical N-bridging ligands were investigated further when the complexes **38a** – **38c** and **39a** – **39c** were synthesized. **38a** – **38c** and **39a** – **39c** all have organic redox active 2,3,5,6-tetra(2-pyridyl)pyrazinyl (tppz) bridging ligand (Fig. 18).³¹

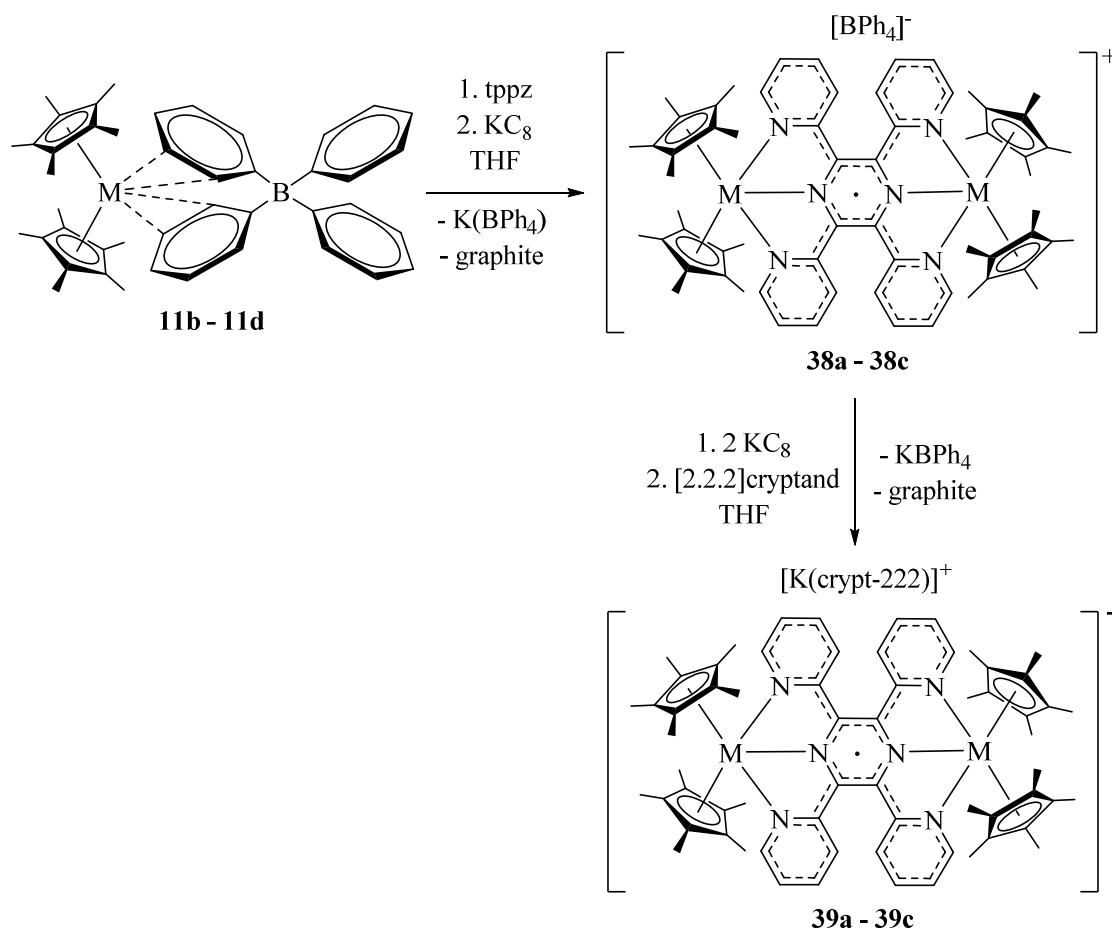


Figure 18. Reaction route for the complexes [(Cp*₂M)₂(μ-η³:η³-tppz^{•-})] [BPh₄], where M = Gd (**38a**), Tb (**38b**) or Dy (**38c**) and [K(crypt-222)][(Cp*₂M)₂(μ-η³:η³-tppz^{•3-})], where M = Gd (**39a**), Tb (**39b**) or Dy (**39c**).³¹

The syntheses of **38a** – **38c** were very similar to the syntheses of complexes **37a** – **37c**. The complexes **39a** – **39c** were obtained by adding KC₈ and [2.2.2]Cryptand to the THF solutions of **38a** – **38c**. In the two sets of products the redox active bridging tppz- ligands have different oxidation states. Radical tppz^{•-} in **38a** – **38c** is in monoanionic form and tppz^{•3-} in **39a** – **39c** is in trianionic form. Two accessible oxidation states of the bridging ligand give opportunity to examine, what effect oxidation states have on the exchange couplings between bridging ligands and lanthanoid centers. Moreover, the bridging ligand with various oxidation states allows the tuning of complex magnetic properties without changing its coordination environment.³¹

M-tppz[•] exchange coupling constants were determined for **38a** and **39a** to be $J = -6.91 \text{ cm}^{-1}$ and $J = -6.29 \text{ cm}^{-1}$, respectively, which both refer to the antiferromagnetic couplings of the

spins. The most interesting thing in the J -values is that they are of similar magnitude despite the different oxidation states of bridging ligands. Complexes **38b** and **38c** show SMM behavior under a zero applied dc field, but **39b** and **39c** do not. The magnetic anisotropy barriers for **38a** and **39a** were $U_{eff} = 5.1 \text{ cm}^{-1}$ and $U_{eff} = 35.9 \text{ cm}^{-1}$ respectively. They both are much smaller than the U_{eff} values of the bpym-bridged complexes **37b** and **37c**. One reason for this might be that the bpym is a planar ligand and tppz is not. Despite very similar coupling constants the oxidation state of bridging ligand had large effect on magnetic properties of complexes.³¹

3.3.2. Dinuclear complexes with various bridging ligands

Indigo is also a redox active bridging ligand with various accessible oxidation states. Indigo is also a hard donor bridging ligand, as it coordinates to lanthanoid center via oxygen and nitrogen atoms. The complexes $[(\eta^5\text{-Cp}^*)_2\text{M}]_2(\mu\text{-ind})^{n-}$ with charge $n = 0$ (**41a** and **41b**), 1 (**42a** and **42b**) or 2 (**43a** and **43b**) were synthesized in 2017 (Fig. 19).³²

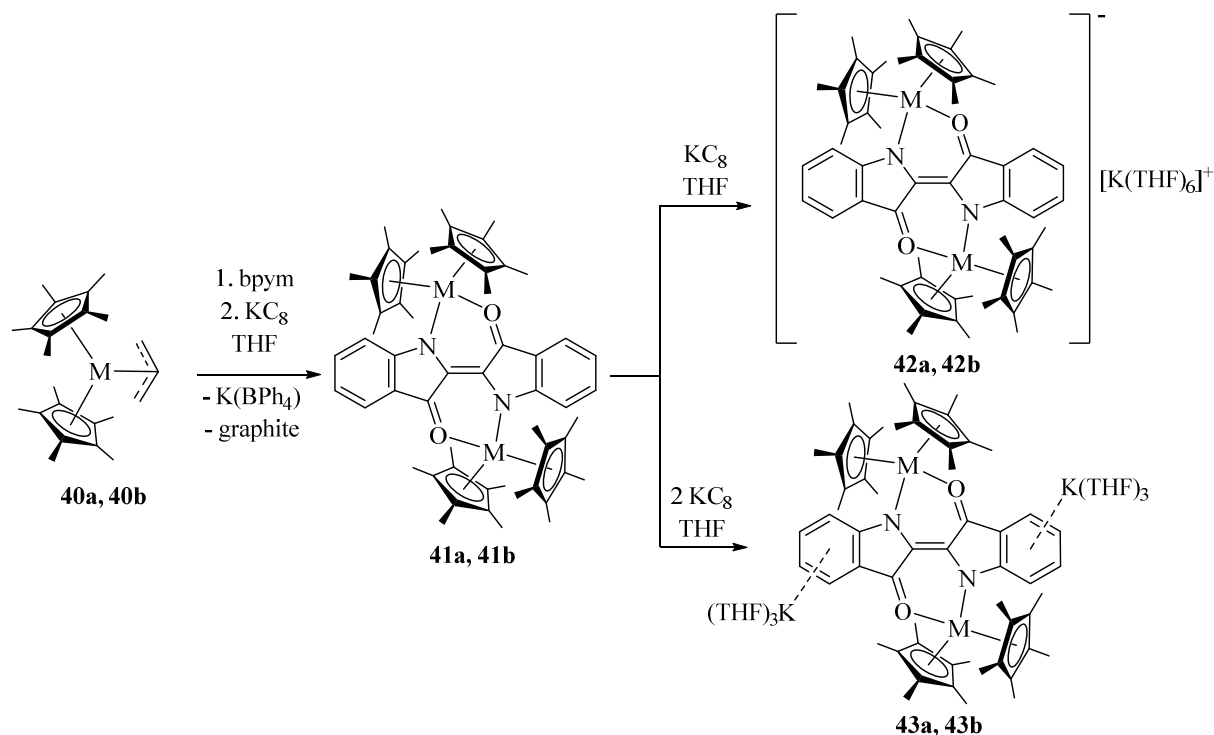


Figure 19. Reaction route for complexes $[(\text{Cp}^*_2\text{M})_2(\mu\text{-ind})]$, where $\text{M} = \text{Gd}$ (**41a**) or Dy (**41b**), $[(\text{Cp}^*_2\text{M})_2(\mu\text{-ind})]^-$, where $\text{M} = \text{Gd}$ (**42a**) or Dy (**42b**) and $[(\text{Cp}^*_2\text{M})_2(\mu\text{-ind})]^{2-}$, where $\text{M} = \text{Gd}$ (**43a**) or Dy (**43b**).³²

Synthetically interesting in reactions, besides the use of indigo as a bridging ligand in the lanthanoid complexes, is that the [2.2.2]Cryptand was not used with KC_8 in the redox reactions. Instead of [2.2.2]Cryptand, THF complexed with K^+ as $[\text{K}(\text{thf})_6]^+$ in **42a** and **42b**

and as $[\text{K}(\text{thf})_3]^+$ in **43a** and **43b**. In the radical bridged complexes **42a** and **42b** the $[\text{K}(\text{thf})_6]^+$ cation appears in the crystal structure as a separate ion, but in the complexes **43a** and **43b** the two $[\text{K}(\text{thf})_3]^+$ cations are coordinated to the lanthanoid complexes via cation- π interaction between the cation and aromatic rings of indigo. Complexes of Gd^{3+} are very similar to their Dy^{3+} analogues, but the bond distances and angles varied with oxidation state of the complexes. The intramolecular $\text{Dy}\cdots\text{Dy}$ distances decreased from 7.078 Å to 6.921 Å and 6.874 Å when charge of the complexes, **41b**, **42b** and **43b**, respectively, increased.³²

The Gd-Gd exchange coupling constants were determined for Gd- complexes **41a**, and **43a** to be $J = -0.013 \text{ cm}^{-1}$, and $J = -0.018 \text{ cm}^{-1}$ respectively, indicating that they both have very weak antiferromagnetic couplings. The weak magnitude of couplings in the complexes **41a** and **43a** are typical for Gd^{3+} - complexes. The Gd-ind exchange coupling constant was determined for the radical bridged complex **42a** to be $J = -11.04 \text{ cm}^{-1}$. The exchange coupling constant for **42a** refers to an unusually strong antiferromagnetic coupling and was the second highest for any radical bridged lanthanoid complex in 2017. Magnetic properties of all Dy^{3+} complexes were measured. Ac magnetic susceptibility measurements confirmed that **41b** and **42b** are SMMs, but **43b** is not. Magnetic anisotropy barriers for complexes **41b** and **42b** were determined to be $U_{\text{eff}} = 39 \text{ cm}^{-1}$ and $U_{\text{eff}} = 35 \text{ cm}^{-1}$, respectively. The U_{eff} values are quite small for the Dy^{3+} complexes. This can be partly explained by the structures of complexes. Equatorially oriented indigo ligand includes oxygen and nitrogen atoms that act as hard donor atoms strengthening the equatorial ligand field around oblate Dy^{3+} - ion. This would also explain, why **43b** is not an SMM. High formal charge of -4 on the indigo- ligand creates a strong electrostatic Dy-ind interaction that leads to the rapid relaxation of magnetization. The study indicated that the axial ligand field created by cyclopentadienyls and the antiferromagnetic exchange between the lanthanoid centers and radical bridging ligand is not enough to create good SMMs if the equatorial ligand field is too strong.³²

Considerably different approach to synthesis of new lanthanoid complexes was the use of isocarbonyl bridging ligand ($\mu\text{-(OC)}_2\text{FeCp}$) in making the new dinuclear trivalent SMM **44** (Fig. 20).³³

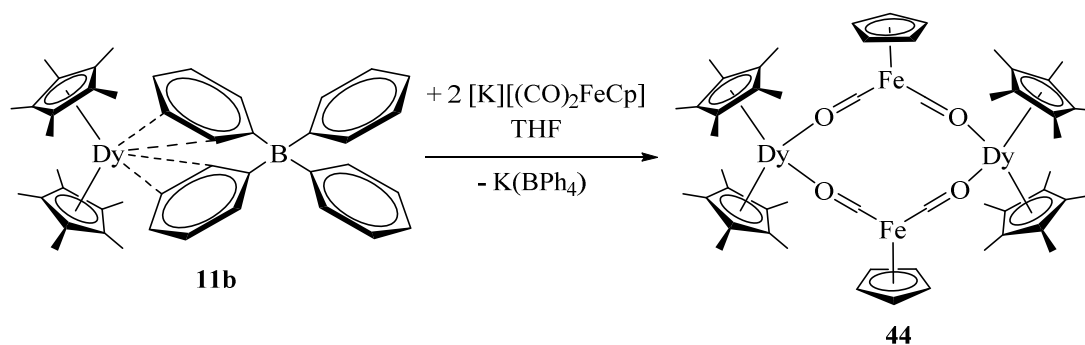


Figure 20. Reaction route for the complex $[\text{DyCp}^*_2(\mu\text{-}(\text{OC})_2\text{FeCp})_2]$ (**44**).³³

The complex $\text{Cp}^*_2\text{Dy}(\mu\text{-Ph}_2)\text{BPh}_2$ is a common starting material in lanthanoid syntheses, as discussed above, but linear isocarbonyl ligands with iron atoms as hard donors appear to be effective way of approaching SMMs with large magnetic anisotropy barriers. Indeed, the complex **44** was reported to have the anisotropy barrier of $U_{\text{eff}} = 662 \text{ cm}^{-1}$, which was the second highest for any SMM reported by 2016. The exceptionally high U_{eff} can be explained with the crystal structure of **44**. In the crystal structure Cnt-Dy-Cnt bond angle between Dy^{3+} and Cp^* :s coordinated to it was 141.5° , which was 11° larger than any analogous angle in Cp_2Dy - based SMMs before. This was enabled by non-bulky isocarbonyl ligands, that do not force Cp^* - ligands to push closer to each other. The Cnt-Dy-Cnt bond angle with short enough Cnt-Dy distance and electron density donation from the Fe-atoms of the bridging ligands resulted to the high U_{eff} . The example demonstrates the importance of ligand field geometry to magnetic properties of dysprosium metallocenium based SMMs.³³

Unlike nitrogen and oxygen containing bridging ligands, bridging Cl^- is a soft donor ligand making it interesting subject in the field of Ln-SMMs. Soft donor ligands and p-block elements other than carbon, oxygen and nitrogen were uncommon bridging ligands in Ln-SMMs for a long time. In 2012 a non-bulky Cl^- bridging ligand was used in Ln-SMMs **45a**, **45b** and **46** (Fig. 21).

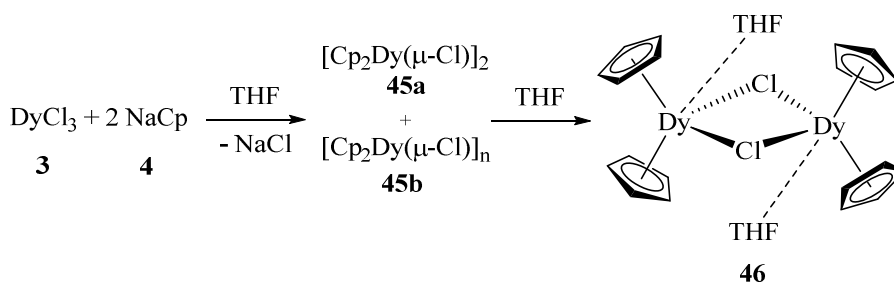


Figure 21. Reaction route for the complexes $[\text{Cp}_2\text{Dy}(\mu\text{-Cl})]_n$, where $n = 2$ (**45a**) or ∞ (**45b**) and $[\text{Cp}_2(\text{thf})\text{Dy}(\mu\text{-Cl})]_2$ (**46**).³⁴

The complexes **45a** and **45b** are just two different polymorphs of same compound, which crystallize as separate crystals as they are purified via a sublimation. The crystals of **45a** and **45b** were separated manually and crystal structures were measured and determined separately. The complex **46** was synthesized exposing mixture of **45a** and **45b** to hot THF.

The magnetic properties of all three complexes were measured and all three complexes appeared to be an Ln-SMMs. The magnetic anisotropy barrier of **46** was $U_{eff} = 48.7$ K (~ 33.9 cm^{-1}) and **46** also had an exchange biased quantum tunneling effect. The exchange biased quantum tunneling effect means that interaction between two Dy^{3+} ions produces a small magnetic field in the complex even in the absence of the external magnetic field. Anisotropy barriers for **45a** and **45b** were $U_{eff} = 26.3$ cm^{-1} and $U_{eff} = 67.8$ cm^{-1} respectively. There was also huge difference in the relaxation times of the complexes. The polymer **45b** was reported to have the relaxation time of $\tau = 78.6$ ms, which is 500 times longer than the relaxation time $\tau = 0.15$ ms of the dimer **45a**. The U_{eff} of **45b** was reported to be larger than the U_{eff} of any other homospin Dy polymer SMM in 2012.³⁴

The magnetic properties of **46** were compared magnetic properties of thiolate bridged Dy^{3+} complex **49b** when the complexes **49a** and **49b** were synthesized and examined later in 2012 (Fig. 22).³⁵

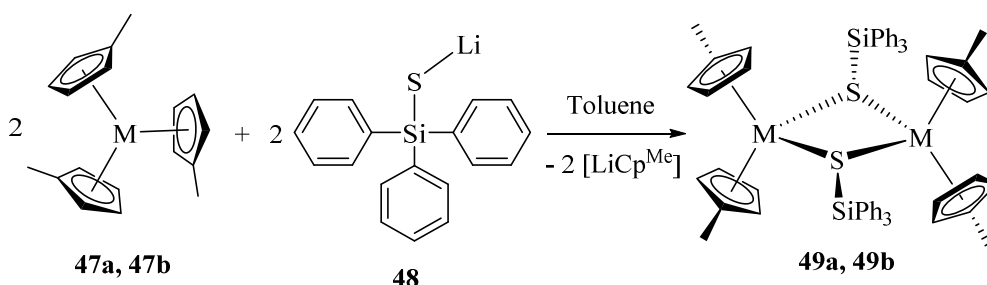


Figure 22. Reaction route for the complexes $[\text{Cp}^{\text{Me}}_2\text{M}(\mu\text{-SSiPh}_3)]_2$, where M = Gd (**49a**) or Dy (**49b**).³⁵

The complexes **49a** and **49b** were synthesized via a simple ligand substitution reaction between $\text{M}(\text{Cp}^{\text{Me}})_3$ and lithiated thiolate ligand. The complexes **49a** and **49b** were crystallized from toluene and the crystal structures and magnetic properties were measured. The Gd^{3+} -complex **49a** was synthesized in order to determine the exchange coupling constant J for it, which was $J = -0.105$ cm^{-1} . The coupling constant indicates the weak antiferromagnetic Gd^{3+} - SSiPh_3 coupling. Magnetic anisotropy barrier of **49b** was $U_{eff} = 133$ cm^{-1} , which was in 2012 the highest barrier reported for a dinuclear Dy^{3+} SMM. The Dy^{3+} - complex **49b** was the first sulfur bridged SMM ever reported.³⁵

The magnetic properties of **49b** were compared to those of **46**, because the complexes had similarities in their structure. The peculiar feature was huge difference in the U_{eff} values of the two complexes. The lower U_{eff} value of **46** was caused by more prominent QTM process than in **49b**. The synthesis and magnetic properties of **49b** indicated that softer donor atoms can be used to boost the SMM properties of Ln-SMMs. Actually, the study prompted further investigation of Ln-SMMs with soft donor atoms.³⁵

3.3.3. Trinuclear Ln-SMMs with pnictogen donor ligands

In addition to **49b**, the bridging ligands containing heavier p-block elements as coordinating atoms were employed in the trinuclear Dy^{3+} complexes **48a** and **49a** (Fig. 23).³⁶

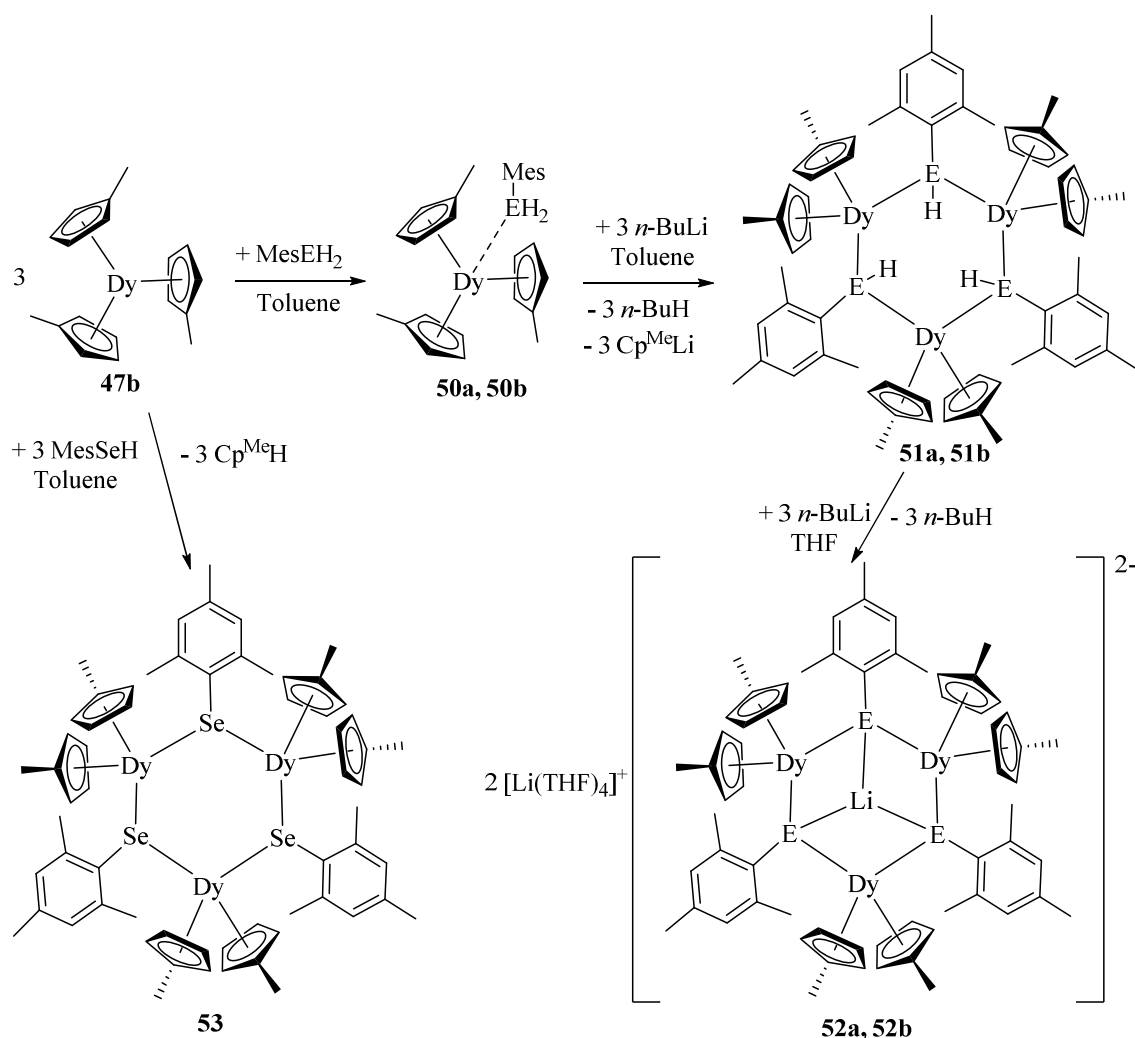


Figure 23. Reaction routes for the complexes $[Cp^{Me_3}Dy(EH_2Mes)]$ (**50a-b**, E = P or As), $[(Cp^{Me_2}Dy)(\mu-E(H)Mes)]_3$ (**51a-b**, E = P or As), $[(Cp^{Me_2}Dy)_3(\mu-EMes)_3Li]^{2-}$ (**52a-b**, E = P or As) and $[(Cp^{Me_2}Dy)(\mu-SeMes)]_3$ (**53**).³⁶

The phosphorus bridging ligands were chosen, because P may occur in complexes with different nominal charges, which would affect electronic properties of the whole complex. Also, the coordination environment of P could be altered as illustrated with the synthesis of **52a** from **51a**. The synthetic route to the complex **53a** started from the addition of MesPH₂ to **47b** yielding **50a**. **50a** was then reacted with *n*-BuLi resulting in the cleavage of one Cp^{Me} from each **47a** complexes and formation of **51a**. By deprotonating (μ -PHMes)- ligands of **51a** with three equivalents of *n*-BuLi resulted in the complex **52a**. The syntheses of arsenic complexes, that will be discussed later, were done same way as phosphine ones. Due to the strong proton affinity of cyclopentadienyl, it can cleavage acidic protons like the proton of MesSeH in the synthesis of **53**, where *n*-BuLi was not needed.³⁶

The magnetic properties of **50a**, **51a** and **52a** were measured and complex **51a** was found to be the Ln-SMM with the magnetic anisotropy barrier of $U_{eff} = 210(5) \text{ cm}^{-1}$. Magnetically dilute version of **51a** (**51a'**) with one Dy³⁺- and two Y³⁺- ions had even higher anisotropy barrier of $U_{eff} = 256(6) \text{ cm}^{-1}$. **51a'** was also reported to have the wider hysteresis loop than **51a** had. Differences in the magnetic properties between **51a** and **52a** were studied with quantum chemical calculations. Weaker magnetic properties of **52a** were caused by higher charge of μ -PHMes- ligands, which caused the stronger equatorial ligand field in **52a** than in **51a**. The strengths of ligand fields were visible in crystal structures of **52a** and **51a**. The Dy-P bond lengths in **52a** were on average 0.13 Å shorter than the Dy-P bond lengths in **51a**. The Cnt-Dy-Cnt bond angles between centroids of cyclopentadienyl ligands and Dy³⁺- ions were on average 3.4° smaller in **52a** than in **51a**.³⁶

The complexes **50b**, **51b**, **52b** and **53** in Fig. 23 were synthesized one year later in 2016. Arsenic and selenium in the bridging ligands are both also heavier p-block elements. The magnetic properties of the complexes **50b**, **51b**, **52b** and **53** were measured and the complexes **51b** and **53** appeared to be Ln-SMMs with the magnetic anisotropy barriers of 256(5) cm⁻¹ and 252(4) cm⁻¹, respectively. The U_{eff} values are larger than the U_{eff} of **51a** was. The complex **51b** is also the first Ln-SMM with metalloid donor ligands. The magnetically dilute analogues of **50b**, **51b**, **52b** and **53** (**50b'**, **51b'**, **52b'** and **53'**) were synthesized and they all had slightly larger U_{eff} than the original Dy³⁺ complexes. The hysteresis loops were also wider for the magnetically diluted complexes. Magnetic dilution had the same effect on the complexes, as it had on **51a**. The slightly better magnetic properties of magnetically diluted multinuclear rare-earth complexes are because many paramagnetic lanthanoid ions in the same complex usually have some interactions between each other. The weak magnetic interactions usually lead to weaker magnetic properties. The interactions between the different

paramagnetic lanthanoid ions, like Dy^{3+} ions, are difficult to predict and the best way to investigate them is the magnetic dilution. Diamagnetic Y^{3+} ions do not have magnetic interactions with paramagnetic Dy^{3+} ion. The reasons for **51b** and **53** being SMMs were the same as for **51a**. The strong axial ligand fields around Dy^{3+} centers in **51b** and **53** created the strong magnetic anisotropy and magnetic exchanges between Dy^{3+} centers were enough to improve the slow relaxation of the magnetization. Complex **52b** was reported to have shorter Dy-As bonds than **51b** and **53**, which allowed rapid relaxation path for magnetization in **52b**.³⁷

More trinuclear lanthanoid complexes with metalloids donor ligands were synthesized in 2017. Antimony was used as heavy p-block donor atom in the bridged in complexes **51c** and **52**. The complexes were synthesized from $\text{DyCp}^{\text{Me}}_3$ with *n*-BuLi and mesitylstibine (MesSbH_2) (Fig. 24).³⁸

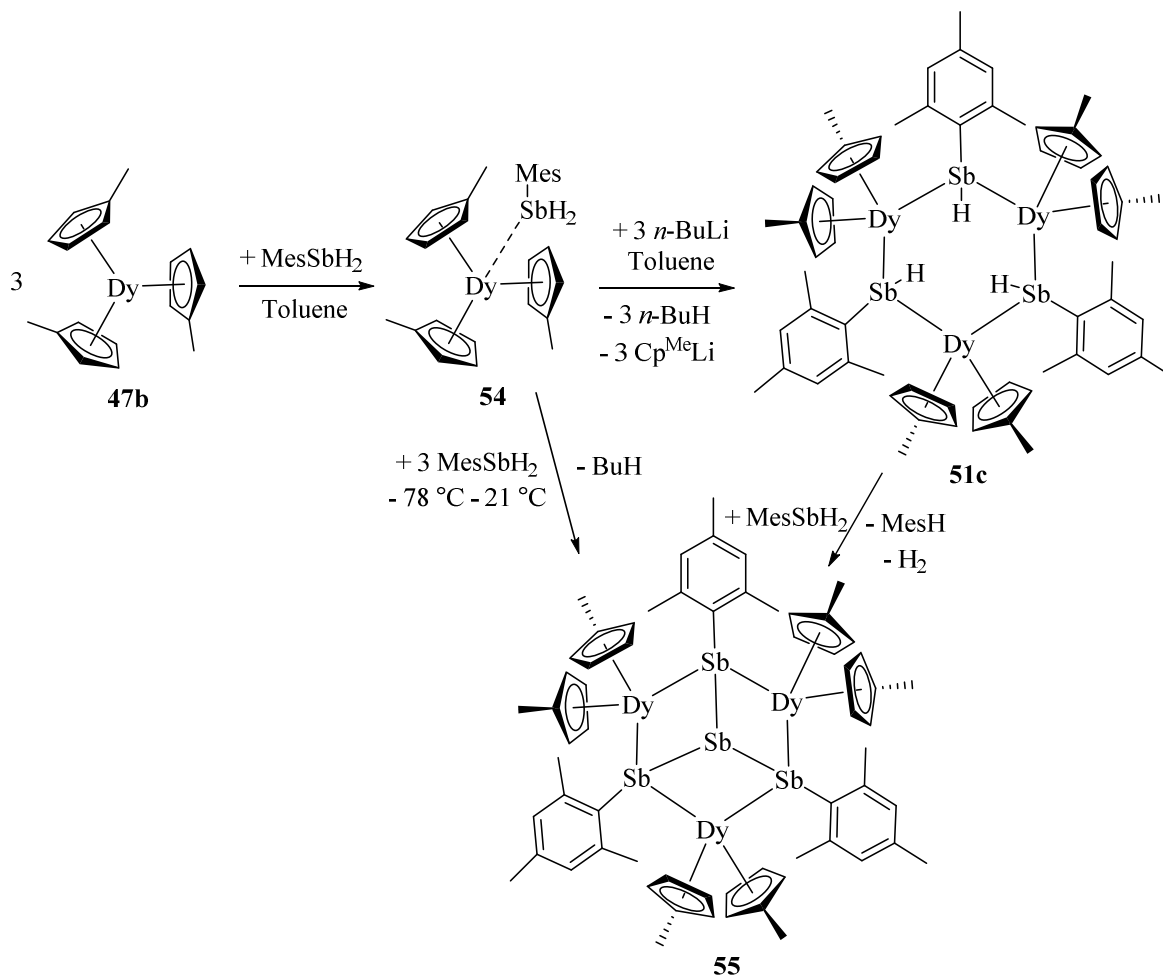


Figure 24. Reaction routes for the complexes $[(\text{Cp}^{\text{Me}}_2\text{Dy})(\mu\text{-Sb(H)Mes})_3]$ (**51c**) and $[(\text{Cp}^{\text{Me}}_2\text{Dy})_3(\mu\text{-SbMes})_3\text{Sb}]$ (**55**).³⁸

The reaction routes for **51c** and **55** were different than those of **51a** and **51b** and required the careful control of temperature. If **54** was mixed with MesSbH_2 and left to the room

temperature for 24 hours, the only isolated products were Sb_4Mes_4 and $\text{Sb}_2\text{H}_2\text{Mes}_2$. The same reaction of **54** and MesSbH_2 was performed with 3:3 ratio in $-50\text{ }^\circ\text{C}$ within 30 min and the main product was **51c**. In synthesis performed with 3:4 ratio of **54** and MesSbH_2 , the main product was **55** as temperature was allowed to rise gradually from $-78\text{ }^\circ\text{C}$ to the room temperature over 12 hours. Alternative way to synthesize **55** was via cross-dehydrocoupling reaction between **51c** and MesSbH_2 . This was reported to be the first time an SMM is produced via such a reaction.³⁸

The magnetic properties of **51c** and **55** were measured and both complexes were confirmed to be Ln-SMMs with the magnetic anisotropy barriers of $U_{\text{eff}} = 345\text{ cm}^{-1}$ and $U_{\text{eff}} = 270\text{ cm}^{-1}$, respectively. The calculated main magnetic axes for each Dy- center in **51c** and **55** were all oriented in the $\text{Cp}^{\text{Me}}\dots\text{Cp}^{\text{Me}}$ directions. Also, the main magnetic axes of **51a** and **51b** had similar orientations. The magnetic hysteresis loops of **51c** and **55** were very narrow, but the magnetic hysteresis loops of their magnetically diluted analogues **51c'** and **55'** were wide. The phenomenon can be explained with dipolar interaction between Dy^{3+} - centers that allows the rapid relaxation of magnetization. The magnetic anisotropy barriers of complexes **51a**, **51b** and **51c** showed rising trend from **51a** ($U_{\text{eff}} = 210\text{ cm}^{-1}$) to **51b** ($U_{\text{eff}} = 256\text{ cm}^{-1}$) and **51c** ($U_{\text{eff}} = 345\text{ cm}^{-1}$) as the radii of the pnictogen atoms in the bridging ligands rises from P to As and Sb. The trend suggests that even higher U_{eff} could be achieved for analogous complexes in which bridging ligands contain even larger p-block elements.³⁸

3.4. Polynuclear hydride bridged complexes

The hydride bridged complexes are synthetically interesting species, because of their high reactivity and synthetic possibilities they offer such as in the synthesis of the complex **22** in Fig. 10. The hydride bridged Cp ligated lanthanoid complexes were studied rigorously in 1980's, but the interest dropped for almost 15 years. During last 15 years there has again been progress in the field of research. The first such complexes were **57a**, **57b** and **57c**. Soon after the publication of the three dinuclear complexes, the two trimetallic hydride complexes **58** and **60** were published. The syntheses and characterizations of complexes **57a** – **57c** and complexes **58** and **60** were all published during 1982 (Fig. 25).^{39,40}

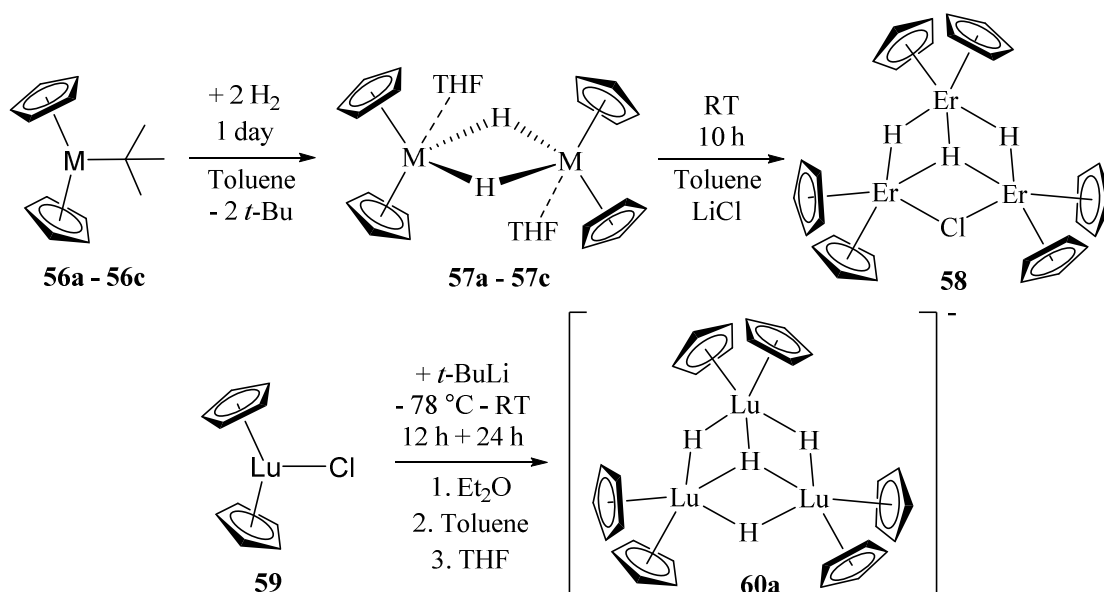


Figure 25. Reaction routes for the complexes [(Cp₂M)(thf)(μ-H)₂], where M = Lu (**57a**), Er (**57b**) or Y (**57c**), [(Cp₂Er)₃(μ-H)₃(μ-Cl)] (**58**) and [(Cp₂Lu)₃(μ-H)₄] (**60a**).^{39,40}

The complexes analogous to **57a** – **57c** were also synthesized with Cp^{Me}- ligands, but Cp ligated **57a** – **57c** are presented here because **58** and **60a** were synthesized originally only with Cp- ligands. The crystal structures and compositions for complexes **57a** – **57c** were well defined, but the structures of complexes **58** and **60a** were not determined unambiguously. Especially the bridging Cl⁻ in crystal structure of **58** had unusually large thermal motion, and Er-Cl bond lengths differed from each other (2.64 Å and 2.74 Å). The structure of **60a** was determined merely with NMR measurements. Despite difficulties with characterizations it was clear, that the first dinuclear and trinuclear hydride bridged organometallic lanthanoid complexes had been synthesized and isolated successfully.^{39,40}

Synthetic routes for Y³⁺ complexes **57c** and [(Cp^{Me}₂Y)₃(μ-H)₄] (**60b**) were investigated and improved in 1984. Both **57c** and **60b** were characterized unambiguously. Y³⁺ was chosen for both dinuclear and trinuclear complexes, because it provides diamagnetic complexes, which can be characterized by NMR spectroscopy. Y³⁺ also allows information about Y-H and Y-C couplings to be collected, because Y has only one naturally occurring NMR active isotope. The improved synthetic route for **57c** uses Cp₂YMe (**61**) as a starting material instead of **56c**. Stirring **61** in solution of 10:1 ratio of toluene and THF under 1 atm pressure of H₂ overnight yields **57c** with 70 % percent yield. 84 % yield was also obtained, when reaction solution was stirred for an additional day under a fresh supply of hydrogen. The original synthetic route for complexes **57a** – **57c** did not work for corresponding Cp^{Me} ligated complexes. Also, the original synthetic route presented in Figure 25 included cooling the reaction mixture to - 78 °C. The synthesis of trimeric **60a** was originally done with only 12 % yield like in Fig. 25.

The improved synthesis of **60b** was achieved by adding *t*-BuLi to THF solution of **57c**. The synthetic route produced complex **60b** with 75 % yield as the temperature was allowed to rise gradually from $-78\text{ }^{\circ}\text{C}$ to $15\text{ }^{\circ}\text{C}$. Although the improved syntheses of **57c** and **60b** were done with Y^{3+} , the synthetic routes of **57c** and **60b** probably work for most of the lanthanoids, because of similarities in ion radii and properties between yttrium and lanthanoids.^{41,42}

The reactivity and synthetic potential of hydride bridged complexes like **57c** and **60b**, especially the Y^{3+} complexes, were studied mainly during 1980's. Bonding in the complexes and their molecular orbitals were studied and explained in 1985. Such complexes were also found to be very sensitive for the right combination of lanthanoid, Cp- ligands and solvents. The key factor is the steric saturation of the complex, which is the combination of the ionic radii of center metal and the size of the ligands. Decreasing the steric saturation by changing Cp^{Me} - ligands of Y- complex **56c** to Cp- ligands decreases the decomposition reactivity of the complex. Whereas, decreasing the steric saturation of **56c** by changing the *tert*-butyl ligand of **56c** to methyl ligand increases the decomposition reactivity of the complex. The reactivities of hydrides were studied also in 2008, when $[\text{Cp}^{\text{Me}}_2\text{M}(\mu\text{-H})_2]$ complexes of Sm^{3+} and La^{3+} were used as starting materials with phenazine ($\text{C}_{12}\text{H}_8\text{N}_2$) producing complexes $[\text{Cp}^{\text{Me}}_2\text{M}]_2(\mu\text{-}\eta^3\text{-}\eta^3\text{-C}_{12}\text{H}_8\text{N}_2)$ for both lanthanoids. Another illustrative example is the reaction of $[\text{Cp}^{\text{Me}}_2\text{M}(\mu\text{-H})_2]$ and diphenyldisulfide ($\text{C}_6\text{H}_5\text{-S-S-C}_6\text{H}_5$) that yield the complexes $[\text{Cp}^{\text{Me}}_2\text{M}(\text{SPh})_2]$ for both Sm^{3+} and La^{3+} . Yield for $[\text{Cp}^{\text{Me}}_2\text{M}(\text{SPh})_2]$ were $\sim 90\%$ for both lanthanoids. The results illustrate that the reactivities of lanthanoid hydrides can be adjusted to fit for each synthetic purpose and that lanthanoid hydrides can be used effectively, for example, in syntheses of dinuclear complexes instead of widely used $[\text{Cp}^{\text{Me}}_2\text{M}][\text{BPh}_4]$ -complexes.⁴³⁻⁴⁶

In 2014 the magnetic properties of dinuclear hydride bridged complexes were examined. Idea for this came from the dinitrogen bridged lanthanoid complexes like **34c** that were good SMMs. Therefore, it was assumed that the structurally reminiscent dinuclear hydride bridged lanthanoid complexes might possess similar SMM properties. The complexes examined were synthesized from $\text{Cp}^*\text{MCH}(\text{CH}_2)_2$ and H_2 (Fig. 26).

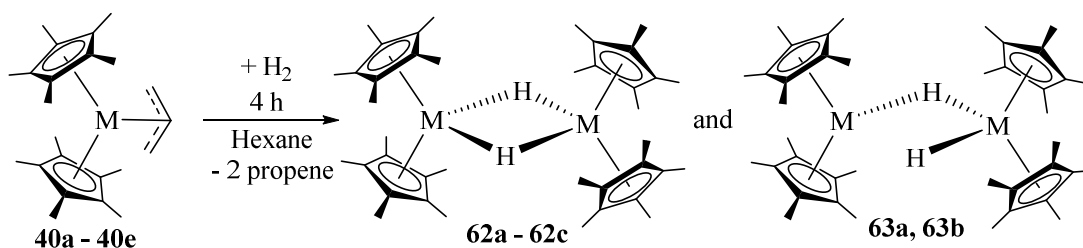


Figure 26. Reaction route for the complexes $[\text{Cp}^*_2\text{M}(\mu\text{-H})]_2$, where $\text{M} = \text{Sm}$ (**62a**), Gd (**62b**) or Tb (**62c**) and $[\text{Cp}^*_2\text{Dy}(\mu\text{-H})\text{MHCp}^*_2]$, where $\text{M} = \text{Dy}$ (**63a**) or Y (**63b**).^{47,48}

The starting materials have propenyl ligand instead of tert-butyl or methyl, but otherwise the reaction route is alike with the previous syntheses reported. The synthetic route was same as presented in 1998 for the synthesis of $[\text{Cp}^*_2\text{Nd}(\mu\text{-H})]_2$. The complexes **62a - 62c**, **63a** and **63b** have Cp^* - ligands instead of Cp or Cp^{Me} . The Cp^* - ligands in the complexes were estimated to be the main reason for the formation of the differently coordinated complexes **63a** and **63b**. **63a** was the complex that could possess SMM properties, but there were problems in the crystallization of **63a**. It crystallized in several different polymorphs and they could not be separated from each other. The crystal structure of **62c** was the only one that was accurate enough for determination of exact places of hydride ligands. The research demonstrated the importance of matching right type of cyclopentadienyl-ligand with right sized lanthanoid.^{47,48}

Hydride bridged rare-earth metal complexes with two different metals in the same complex were synthesized from complexes **62d - 62e** (Fig. 27).

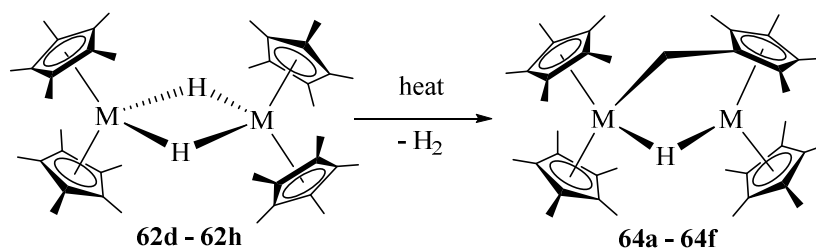


Figure 27. Reaction route for the complexes $\text{Cp}^*_2\text{M}(\mu\text{-H})(\mu\text{-}\eta^1:\eta^5\text{-CH}_2\text{C}_5\text{Me}_4)\text{M}'\text{Cp}^*$ where M/M' were Y/Lu (**64a**), Lu/Y (**64b**), Lu/Lu (**64c**), Y/Y (**64d**), Lu/La (**64e**) or Y/La (**64f**).⁴⁹

The first goal was to identify different metals M and M' , that have reminiscent properties, from each other in the same complex. The second goal was to see, if different ligand environments around metal centers M and M' favor the different sizes of metals ions. Preference for the heterometallic complexes was first observed in the syntheses of **62d - 62h**. Starting materials for their synthesis were the complexes $\text{Cp}^*_2\text{M}(\eta^3\text{-C}_3\text{H}_5)$ (**40e - 40g**), which have only one metal center each. The reaction between the Lu- complex **40e** and the Y- complex **40f** yielded the complexes **62d** (Lu/Y), **62e** (Lu/Lu) and **62f** (Y/Y) in 86:10:4 ratio.

The products could not be isolated, but ratio was calculated from reaction mixture NMR. The reaction between the La- complex **40g** and **40e** and the reaction between **40g** and **40f** yielded only the heterometallic complexes **62g** (Lu/La) and **62h** (Y/La). The larger ions preference for the lower coordination number was observed in the syntheses of the La^{3+} containing complexes **64e** and **64f**. In both reactions, the La^{3+} - ion, with distinctly larger ionic radii than Y^{3+} or Lu^{3+} , favored the site of the lower coordination number, marked as M' in Figure 27. The complexes **64a** - **64d** of metal centers of Lu^{3+} and Y^{3+} with nearly similar ionic radii were successfully isolated, characterized and metal centers determined by NMR spectroscopy.⁴⁹

One uncommon bond type in lanthanoid complexes is the M-M metal bond between lanthanoid ions. Complexes with such a bond would require specific coordinating ligands, because the M-M bond does not form easily due to the contracted 4f-orbitals and large radial size of M^{n+} - ions. The tricky subject was approached in 2017 as the synthesis of the first Y-Y-bonded complexes from hydride bridged $[\text{Cp}^{\text{SiMe}_3}_2\text{Y}(\mu\text{-H})]_2$ and chloride bridged $[\text{Cp}^{\text{SiMe}_3}_2\text{Y}(\mu\text{-Cl})]_2$ complexes was attended. After the Y-Y- complex also the analogous M-M-bonded lanthanoid complexes would be synthesized. The hypothesis of the synthetic route was based on DFT calculations, which predicted the hydride-bridged complexes to be suitable starting materials for the complexes with M-M- bonding between divalent M^{2+} - ions. The configurations of divalent lanthanoids were the key factors in the hypothesis, because divalent lanthanoids may possess $4f^n5d^1$ configurations in suitable ligand environments. $4f^n5d^1$ configurations of lanthanoid ions are required for the formation of the M-M- bond.⁵⁰

Despite the careful calculations, no Y-Y- bonded or M-M- bonded products were isolated from the reaction mixtures. EPR measurements of crude solution of mixed products showed features of M^{2+} - ions, but only isolated products were analogous to **67a** - **67c** with $[\text{K}(\text{Crypt-222})]^+$ or $[\text{K}(18\text{-c-6})]^+$ counter ions (Fig. 28). Despite the lack of desirable products something else was discovered during the research. In the synthesis of dinuclear hydride complexes **66a** - **66c**, the synthesized Y^{3+} complex was trinuclear **67c** instead of dinuclear **66c**. The trinuclear complex was successfully converted to the dinuclear one and dinuclear Dy^{3+} and Tb^{3+} complexes **66a** and **66b** were successfully converted to their corresponding trinuclear complexes **67a** and **67b** (Fig. 28).⁵⁰

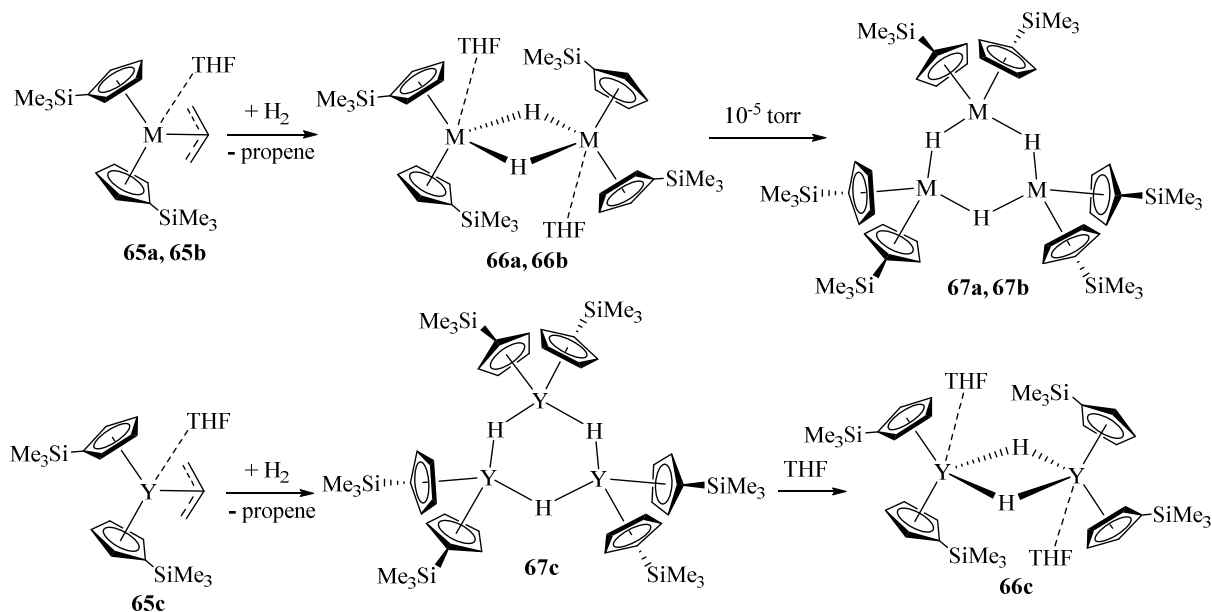


Figure 28. Reaction routes for the complexes $[\text{Cp}^{\text{SiMe}_3}_2\text{M}(\mu\text{-H})(\text{thf})]_2$, where $\text{M} = \text{Dy}$ (**66a**) or Tb (**66b**), $[\text{Cp}^{\text{SiMe}_3}_2\text{M}(\mu\text{-H})]_3$, where $\text{M} = \text{Dy}$ (**67a**) or Tb (**67b**), $[\text{Cp}^{\text{SiMe}_3}_2\text{Y}(\mu\text{-H})(\text{thf})]_2$ (**66c**) and $[\text{Cp}^{\text{SiMe}_3}_2\text{Y}(\mu\text{-H})]_3$ (**67c**).⁵⁰

Determining aspect between the dimeric complexes **66** and trimeric complexes **67** was the amount of THF present. The trimeric Y^{3+} complex **67c** required a larger amount of THF to convert to **66c** than analogous lanthanoid complexes **67a** and **67b** did. These findings were considered to be new synthetic routes for the complexes **66a** - **66c** and **67a** - **67c**, that have $\text{Cp}^{\text{SiMe}_3}$ - ligands instead of previously used Cp -, Cp^{Me} - or Cp^* - ligands.⁵⁰

4. Conclusions

Cp- ligands have been used in lanthanoid complexes for various reasons. Divalent M^{2+} ions were isolated for all lanthanoids and yttrium in the same coordination environment as $[K(2.2.2\text{-Crypt})][\eta^5\text{-Cp}^{\text{SiMe}_3}_3M]$ and the unexpected variation was found in the electronic configurations of divalent lanthanoids. The electronic configurations of trivalent lanthanoids are more clear, but still trivalent lanthanoids show very interesting reactivity like the unexpected reaction between $[\text{Cp}^*\text{Dy}][(\mu\text{-Ph})_2\text{BPh}_2]$, THF and NH_3 to yield $[\text{Cp}^*\text{Dy}(\text{NH}_3)(\text{THF})][\text{BPh}_4]$ (**17**) and the two step reaction from $[\text{Dy}(\text{Cp}^{\text{iPr}_5})(\text{BH}_4)_2(\text{THF})]$ (**20**) to $[(\text{Cp}^{\text{iPr}_5})\text{Dy}(\text{Cp}^*)(\text{BH}_4)]$ (**21**) and to the low coordinated Ln-SMM $[(\text{Cp}^{\text{iPr}_5})\text{Dy}(\text{Cp}^*)]^+$ (**22**).

The combination of Dy^{3+} - ion and strongly axial ligand field has proven its effectiveness in single molecular magnetism. The best examples of such combination are the low coordinated Dy^{3+} metallocenium SMMs **22** and $[\text{B}(\text{C}_6\text{F}_5)_4][(\text{Cp}^{\text{ttt}})_2\text{Dy}]$ (**19**). **22** and **19** are so far the best SMMs among all reported Ln-SMMs as well as **22** is the only SMM that retains its SMM properties above liquid nitrogen temperatures. The excellence of Dy^{3+} - ion in SMMs is based on two main things. The first thing is the Dy^{3+} - ions high magnetic anisotropy that can be boosted with strong axial ligand field. The second thing is the fact that Dy^{3+} is a Kramer's ion, which means that ligand field around Dy^{3+} - ion does not have to be perfectly axial for complex to possess SMM properties. Therefore, the best way to synthesize new Ln-SMMs seems to be using Dy^{3+} - ions with simple axial ligand field like in complexes **22** and **19**. Other ways to produce Ln-SMMs include polynuclear lanthanoid complexes that have the bridging ligands with heteroatoms. The SMM properties of polynuclear complexes are not as good as with low coordinated single ion complexes, but they offer valuable information about the syntheses and reactivity of lanthanoids. Some of those complexes have proven themselves as multielectron reductants. One way of getting better magnetic properties for polynuclear heteroatom bridged complexes have been reducing the bridging ligands to stable radicals to generate a strong enough exchange coupling between the unpaired electron of radical ligand and metal spins to quench the QTM process.

The synthetic versatility of the lanthanoid complexes of cyclopentadienyl ligands (Ln-Cp complexes) has been proved also with various di- and trinuclear hydride bridged complexes. These complexes could be used as catalysts or as starting materials for other types of complexes or MOFs. The reducing power of Ln-Cp complexes has been proven in the syntheses of hydride bridged and $[\text{N}_2]^{2-}$ bridged complexes. A good example of the reducing capability of Ln-Cp complexes is the synthesis of $[(\text{Cp}^*)_2\text{M}]_2(\mu\text{-}\eta^2\text{:}\eta^2\text{-N}_2)$ (**34b**), where the

starting material $[(\text{Cp}^*)_2\text{Lu}(\eta^3\text{-Cp}^{\text{Me}4})]$ (**33b**) was reactive enough to reduce usually inert N_2 gas by photochemical activation without other reducing agents. The Ln-Cp complexes possess interesting and very useful catalytic and synthetic properties, but today the focus in their research is in developing the new and better Ln-SMMs.

Possible future applications of Ln-SMMs are in molecular spintronics and even in the quantum computing as more and better Ln-SMMs, that retain their slow relaxation of magnetization in practical temperatures, are developed. The Ln-Cp complexes have future potential also in the synthetic field. Carefully planned synthetic routes with reactive Ln-Cp complexes as starting materials offer a chance to synthesize the new Ln- complexes and Ln-SMMs with no other reducing agents or catalysts.

List of References

- (1) Wilkinson, G., Birmingham, J. M., Cyclopentadienyl Compounds of Sc, Y, La, Ce and Some Lanthanide Elements, *J. Am. Chem. Soc.*, **1954**, 76 (23), 6210–6211.
- (2) Goodwin, C. A. P., Ortu, F., Reta, D., Chilton, N. F., Mills, D. P., Molecular Magnetic Hysteresis at 60 Kelvin in Dysprosocenium, *Nature*, **2017**, 548 (7668), 439–442.
- (3) Guo, F. S., Day, B. M., Chen, Y. C., Tong, M. L., Mansikkamäki, A., Layfield, R. A., A Dysprosium Metallocene Single-Molecule Magnet Functioning at the Axial Limit, *Angew. Chemie - Int. Ed.*, **2017**, 56 (38), 11445–11449.
- (4) Guo, F.-S., Day, B. M., Chen, Y.-C., Tong, M.-L., Mansikkamäki, A., Layfield, R. A., Magnetic Hysteresis up to 80 Kelvin in a Dysprosium Metallocene Single-Molecule Magnet, *Science*, **2018**, 362 (6421), 1400–1403.
- (5) Day, B. M., Guo, F. S., Layfield, R. A., Cyclopentadienyl Ligands in Lanthanide Single-Molecule Magnets: One Ring to Rule Them All?, *Acc. Chem. Res.*, **2018**, 51 (8), 1880–1889.
- (6) Housecroft, C. E., Sharpe, A. G., *Inorganic Chemistry*, 4th ed., Pearson Education Limited, Harlow, **2012**.
- (7) Fieser, M. E., Bates, J. E., Furche, F., Evans, W. J., Krull, B. T., Ziller, J. W., MacDonald, M. R., Structural, Spectroscopic, and Theoretical Comparison of Traditional vs Recently Discovered Ln²⁺ Ions in the [K(2.2.2-Cryptand)][(C₅H₄SiMe₃)₃Ln] Complexes: The Variable Nature of Dy²⁺ and N, *J. Am. Chem. Soc.*, **2014**, 137 (1), 369–382.
- (8) Shannon, R. D., Revised Effective Ionic Radii and Systematic Studies of Interatomic Distances in Halides and Chalcogenides, *Acta Crystallogr. Sect. A*, **1976**, 32 (5), 751–767.
- (9) MacDonald, M. R., Ziller, J. W., Evans, W. J., Synthesis of a Crystalline Molecular Complex of Y²⁺, [(18-Crown-6)K][(C₅H₄SiMe₃)₃Y], *J. Am. Chem. Soc.*, **2011**, 133 (40), 15914–15917.
- (10) Woodruff, D. N., Winpenny, R. E. P., Layfield, R. A., Lanthanide Single-Molecule Magnets, *Chem. Rev.*, **2013**, 113 (7), 5110–5148.
- (11) Birmingham, J. M., Wilkinson, G., The Cyclopentadienides of Scandium, Yttrium and

- Some Rare Earth Elements, *J. Am. Chem. Soc.*, **1956**, 78 (1), 42–44.
- (12) Mansikkamäki, A., *Theoretical And Computational Studies Of Magnetic Anisotropy And Exchange Coupling In Molecular Systems*, University of Jyväskylä, Department of Chemistry, Research Report No. 207, Jyväskylä, **2018**.
- (13) Rinehart, J. D., Long, J. R., Exploiting Single-Ion Anisotropy in the Design of f-Element Single-Molecule Magnets, *Chem. Sci.*, **2011**, 2 (11), 2078–2085.
- (14) Fischer, E. O., Fischer, H., Über Dicyclopentadienyleuropium Und Dicyclopentadienylterbium Und Tricyclopentadienyle Des Terbiums, Holmiums, Thuliums Und Lutetiums, *J. Organomet. Chem.*, **1965**, 3 (3), 181–187.
- (15) MacDonald, M. R., Bates, J. E., Fieser, M. E., Ziller, J. W., Furche, F., Evans, W. J., Expanding Rare-Earth Oxidation State Chemistry to Molecular Complexes of Holmium(II) and Erbium(II), *J. Am. Chem. Soc.*, **2012**, 134 (20), 8420–8423.
- (16) Hitchcock, P. B., Lappert, M. F., Maron, L., Protchenko, A. V., Lanthanum Does Form Stable Molecular Compounds in the +2 Oxidation State, *Angew. Chemie - Int. Ed.*, **2008**, 47 (8), 1488–1491.
- (17) MacDonald, M. R., Bates, J. E., Ziller, J. W., Furche, F., Evans, W. J., Completing the Series of +2 Ions for the Lanthanide Elements: Synthesis of Molecular Complexes of Pr^{2+} , Gd^{2+} , Tb^{2+} , and Lu^{2+} , *J. Am. Chem. Soc.*, **2013**, 135 (26), 9857–9868.
- (18) Meyer, G., Reduced Halides of the Rare-Earth Elements, *Chem. Rev.*, **1988**, 88 (1), 93–107.
- (19) Fieser, M. E., Long, J. R., Corbey, J. F., Evans, W. J., Meihaus, K. R., Record High Single-Ion Magnetic Moments Through $4f^n 5d^1$ Electron Configurations in the Divalent Lanthanide Complexes $[(\text{C}_5\text{H}_4\text{SiMe}_3)_3\text{Ln}]^-$, *J. Am. Chem. Soc.*, **2015**, 137 (31), 9855–9860.
- (20) Kotyk, C. M., Fieser, M. E., Palumbo, C. T., Ziller, J. W., Darago, L. E., Long, J. R., Furche, F., Evans, W. J., Isolation of +2 Rare Earth Metal Ions with Three Anionic Carbocyclic Rings: Bimetallic Bis(Cyclopentadienyl) Reduced Arene Complexes of La^{2+} and Ce^{2+} Are Four Electron Reductants, *Chem. Sci.*, **2015**, 6 (12), 7267–7273.
- (21) Evans, W. J., Perotti, J. M., Ziller, J. W., Synthetic Utility of $[(\text{C}_5\text{Me}_5)_2\text{Ln}][(\mu\text{-Ph})_2\text{BPh}_2]$ in Accessing $[(\text{C}_5\text{Me}_5)_2\text{LnR}]_x$ Unsolvated Alkyl Lanthanide Metallocenes,

- Complexes with High C–H Activation Rea, *J. Am. Chem. Soc.*, **2005**, *127* (11), 3894–3909.
- (22) Macdonald, M. R., Ziller, J. W., Evans, W. J., Coordination and Reductive Chemistry of Tetraphenylborate Complexes of Trivalent Rare Earth Metallocene Cations, $[(C_5Me_5)_2Ln][(\mu-Ph)_2BPh_2]$, *Inorg. Chem.*, **2011**, *50* (9), 4092–4106.
- (23) Singh, U. P., Tyagi, S., Sharma, C. L., Görner, H., Weyhermüller, T., Synthesis, Molecular Structure and Emission Properties of Benzoato-Bridged Lanthanide Complexes with Hydrotris(Pyrazolyl)Borate, *J. Chem. Soc. Dalton Trans.*, **2002**, No. 23, 4464–4470.
- (24) Demir, S., Boshart, M. D., Corbey, J. F., Woen, D. H., Gonzalez, M. I., Ziller, J. W., Meihaus, K. R., Long, J. R., Evans, W. J., Slow Magnetic Relaxation in a Dysprosium Ammonia Metallocene Complex, *Inorg. Chem.*, **2017**, *56* (24), 15049–15056.
- (25) Layfield, R. A., Bashall, A., McPartlin, M., Rawson, J. M., Wright, D. S., A Structural and Magnetic Study of Organolanthanide(III) Amides, *Dalt. Trans.*, **2006**, No. 13, 1660–1666.
- (26) Layfield, R. A., McDouall, J. J. W., Sulway, S. A., Tuna, F., Collison, D., Winpenny, R. E. P., Influence of the N-Bridging Ligand on Magnetic Relaxation in an Organometallic Dysprosium Single-Molecule Magnet, *Chem. - A Eur. J.*, **2010**, *16* (15), 4442–4446.
- (27) Evans, W. J., Lee, D. S., Johnston, M. A., Ziller, J. W., The Elusive $(C_5Me_4H)_3Lu$: Its Synthesis and $LnZ_3/K/2$ Reactivity, *Organometallics*, **2005**, *24* (4), 6393–6397.
- (28) Fieser, M. E., Bates, J. E., Ziller, J. W., Furche, F., Evans, W. J., Dinitrogen Reduction via Photochemical Activation of Heteroleptic Tris(Cyclopentadienyl) Rare-Earth Complexes, *J. Am. Chem. Soc.*, **2013**, *135* (10), 3804–3807.
- (29) Demir, S., Gonzalez, M. I., Darago, L. E., Evans, W. J., Long, J. R., Giant Coercivity and High Magnetic Blocking Temperatures for N_2^{3-} Radical-Bridged Dilanthanide Complexes upon Ligand Dissociation, *Nat. Commun.*, **2017**, *8* (1), 1–9.
- (30) Demir, S., Zadrozny, J. M., Nippe, M., Long, J. R., Exchange Coupling and Magnetic Blocking in Bipyrimidyl Radical-Bridged Dilanthanide Complexes, *J. Am. Chem. Soc.*, **2012**, *134* (45), 18546–18549.

- (31) Demir, S., Nippe, M., Gonzalez, M. I., Long, J. R., Exchange Coupling and Magnetic Blocking in Dilanthanide Complexes Bridged by the Multi-Electron Redox-Active Ligand 2,3,5,6-Tetra(2-Pyridyl)Pyrazine, *Chem. Sci.*, **2014**, 5 (12), 4701–4711.
- (32) Guo, F.-S., Layfield, R. A., Strong Direct Exchange Coupling and Single-Molecule Magnetism in Indigo-Bridged Lanthanide Dimers, *Chem. Commun.*, **2017**, 53 (21), 3130–3133.
- (33) Pugh, T., Chilton, N. F., Layfield, R. A., A Low-Symmetry Dysprosium Metallocene Single-Molecule Magnet with a High Anisotropy Barrier, *Angew. Chemie - Int. Ed.*, **2016**, 55 (37), 11082–11085.
- (34) Sulway, S. A., Layfield, R. A., Tuna, F., Wernsdorfer, W., Winpenny, R. E. P., Single-Molecule Magnetism in Cyclopentadienyl-Dysprosium Chlorides, *Chem. Commun.*, **2012**, 48 (10), 1508–1510.
- (35) Tuna, F., Smith, C. A., Bodensteiner, M., Ungur, L., Chibotaru, L. F., McInnes, E. J. L., Winpenny, R. E. P., Collison, D., Layfield, R. A., A High Anisotropy Barrier in a Sulfur-Bridged Organodysprosium Single-Molecule Magnet, *Angew. Chemie - Int. Ed.*, **2012**, 51 (28), 6976–6980.
- (36) Pugh, T., Tuna, F., Ungur, L., Collison, D., McInnes, E. J. L., Chibotaru, L. F., Layfield, R. A., Influencing the Properties of Dysprosium Single-Molecule Magnets with Phosphorus Donor Ligands, *Nat. Commun.*, **2015**, 6 (May), 1–8.
- (37) Pugh, T., Vieru, V., Chibotaru, L. F., Layfield, R. A., Magneto-Structural Correlations in Arsenic- and Selenium-Ligated Dysprosium Single-Molecule Magnets, *Chem. Sci.*, **2016**, 7 (3), 2128–2137.
- (38) Pugh, T., Chilton, N. F., Layfield, R. A., Antimony-Ligated Dysprosium Single-Molecule Magnets as Catalysts for Stibine Dehydrocoupling, *Chem. Sci.*, **2017**, 8 (3), 2073–2080.
- (39) Evans, W. J., Meadows, J. H., Wayda, A. L., Hunter, W. E., Atwood, J. L., Organolanthanide Hydride Chemistry. 2. Synthesis and X-Ray Crystallographic Characterization of a Trimetallic Organolanthanide Polyhydride Complex, *J. Am. Chem. Soc.*, **1982**, 104 (7), 2015–2017.
- (40) Evans, W. J., Meadows, J. H., Wayda, A. L., Hunter, W. E., Atwood, J. L., Organolanthanide Hydride Chemistry. 1. Synthesis and X-Ray Crystallographic

- Characterization of Dimeric Organolanthanide and Organoyttrium Hydride Complexes, *J. Am. Chem. Soc.*, **1982**, *104* (7), 2008–2014.
- (41) Evans, W. J., Meadows, J. H., Hunter, W. E., Atwood, J. L., Organolanthanide and Organoyttrium Hydride Chemistry. 5. Improved Synthesis of $[(C_5H_4R)_2YH(THF)]_2$ Complexes and Their Reactivity with Alkenes, Alkynes, 1,2-Propadiene, Nitriles, and Pyridine, Including Structure, *J. Am. Chem. Soc.*, **1984**, *106* (5), 1291–1300.
- (42) Evans, W. J., Meadows, J. H., Hanusa, T. P., Organolanthanide and Organoyttrium Hydride Chemistry. 6. Direct Synthesis and 1H NMR Spectral Analysis of the Trimetallic Yttrium and Yttrium-Zirconium Tetrahydride Complexes, $\{[(C_5H_5)_2YH]_3H\}\{Li(THF)_4\}$ and $\{[(CH_3C_5H_4)_2YH]_2[(CH_3C_5H_4)_2ZrH]H\}$, *J. Am. Chem. Soc.*, **1984**, *106* (16), 4454–4460.
- (43) Ortiz, J. V., Hoffmann, R., Hydride Bridges between $LnCp_2$ Centers, *Inorg. Chem.*, **1985**, *24* (13), 2095–2104.
- (44) Evans, W. J., Dominguez, R., Hanusa, T. P., Structure and Reactivity Studies of Bis(Cyclopentadienyl) Ytterbium and Yttrium Alkyl Complexes Including the X-Ray Crystal Structure of $(C_5H_5)_2Yb(CH_3)(THF)$, *Organometallics*, **1986**, *5* (2), 263–270.
- (45) Evans, W. J., Grate, J. W., Doedens, R. J., Reaction of the Samarium-Hydrogen Bond in $[(C_5Me_5)_2SmH]_2$ with Carbon Monoxide: Formation, Isomerization, and X-Ray Crystallographic Characterization of Cis- and Trans- $\{(C_5Me_5)_2[(C_6H_5)_3PO]Sm\}_2(\mu-OCH=CHO)$, *J. Am. Chem. Soc.*, **1985**, *107* (6), 1671–1679.
- (46) Evans, W. J., Schmiede, B. M., Lorenz, S. E., Miller, K. A., Champagne, T. M., Ziller, J. W., DiPasquale, A. G., Rheingold, A. L., Reductive Reactivity of the Organolanthanide Hydrides, $[(C_5Me_5)_2LnH]_x$, Leads to Ansa-Allyl Cyclopentadienyl ($\eta^5-C_5Me_4CH_2-C_5Me_4CH_2-\eta^3$) $^{2-}$ and Trianionic Cyclooctatetraenyl (C_8H_7) $^{3-}$ Ligands, *J. Am. Chem. Soc.*, **2008**, *130* (26), 8555–8563.
- (47) Evans, W. J., Seibel, C. A., Ziller, J. W., Unsolvated Lanthanide Metallocene Cations $[(C_5Me_5)_2Ln][BPh_4]$: Multiple Syntheses, Structural Characterization, and Reactivity Including the Formation of $(C_5Me_5)_3Nd$, *J. Am. Chem. Soc.*, **1998**, *120* (27), 6745–6752.
- (48) Liu, S.-S., Gao, S., Ziller, J. W., Evans, W. J., Structural Complexity in the Rare Earth Metallocene Hydride Complexes, $[(C_5Me_5)_2LnH]_2$, *Dalt. Trans.*, **2014**, *43* (41), 15526–

15531.

- (49) Fieser, M. E., Mueller, T. J., Bates, J. E., Ziller, J. W., Furche, F., Evans, W. J., Differentiating Chemically Similar Lewis Acid Sites in Heterobimetallic Complexes: The Rare-Earth Bridged Hydride $(C_5Me_5)_2Ln(\mu-H)_2Ln'(C_5Me_5)_2$ and Tuckover Hydride $(C_5Me_5)_2Ln(\mu-H)(\mu-\eta^1:\eta^5-CH_2C_5Me_4)Ln'(C_5Me_5)$ Systems, *Organometallics*, **2014**, 33 (14), 3882–3890.
- (50) Dumas, M. T., Chen, G. P., Hu, J. Y., Nascimento, M. A., Rawson, J. M., Ziller, J. W., Furche, F., Evans, W. J., Synthesis and Reductive Chemistry of Bimetallic and Trimetallic Rare-Earth Metallocene Hydrides with $(C_5H_4SiMe_3)^{1-}$ Ligands, *J. Organomet. Chem.*, **2017**, 849–850, 38–47.